Meiotic chromosome organization and its role in recombination and cancer

Chris Morgan[1#], Aditya Nayak[2#], Noriko Hosoya[3], Gerald R. Smith[4], Christophe Lambing[5*]

[1] John Innes Centre, Colney Lane, Norwich, UK.

[2] Institute of Molecular Plant Biology, Department of Biology, Swiss Federal Institute of Technology (ETH) Zurich, Switzerland

[3] Laboratory of Molecular Radiology, Center for Disease Biology and Integrative Medicine, Graduate School of Medicine, The University of Tokyo, Tokyo, Japan

[4] Division of Basic Sciences, Fred Hutchinson Cancer Research Center, Seattle, USA.

[5] Plant Sciences Department, Rothamsted Research, Harpenden, United Kingdom.

[#] These authors contributed equally to this work.

[*] Corresponding author: christophe.lambing@rothamsted.ac.uk

Abstract

Chromosomes adopt specific conformations to regulate various cellular processes. A well-documented chromosome configuration is the highly compacted chromosome structure during metaphase. More regional chromatin conformations have also been reported, including topologically associated domains encompassing mega-bases of DNA and local chromatin loops formed by kilo-bases of DNA. In this review, we discuss the changes in chromatin conformation taking place between somatic and meiotic cells, with a special focus on the establishment of a proteinaceous structure, called the chromosome axis, at the beginning of meiosis. The chromosome axis is essential to support key meiotic processes such as chromosome pairing, homologous recombination, and balanced chromosome segregation to transition from a diploid to a haploid stage. We review the role of the chromosome axis in meiotic chromatin organization and provide a detailed description of its protein composition.

We also review the conserved and distinct roles between species of axis proteins in meiotic recombination, which is a major factor contributing to the creation of genetic diversity and genome evolution. Finally, we discuss situations where the chromosome axis is deregulated and evaluate the effects on genome integrity and the consequences from protein deregulation in meiocytes exposed to heat stress, and aberrant expression of genes encoding axis proteins in mammalian somatic cells associated with certain types of cancers.

Key words: Meiosis, meiotic recombination, chromosome axis, synaptonemal complex, chromatin, crossover interference, heat stress, cancer.

1. Chromatin and chromosome organization during meiosis

Meiosis is a specialized type of cell division essential for sexual reproduction. Meiosis consists of one round of DNA replication followed by two sequential events of chromosome segregation: the segregation of homologous chromosomes in meiosis I, and the segregation of sister centromeres and their attached chromosomal arms in meiosis II. The two rounds of chromosome segregation are central to transitioning from a diploid to a haploid stage. Proper chromosome segregation depends on the formation of a physical link between two homologous chromosomes (Kuo et al. 2021). In early meiosis, a topoisomerase-like complex forms DNA double-strand breaks (DSBs) that are repaired by homologous recombination. DSBs are resected to form single-strand DNA (ssDNA) molecules that can invade the sister chromatid or the homologous chromosome. ssDNAs anneal with the homologous chromosome to form heteroduplex structures. These structures can be stabilised to form a crossover (CO) which consists of the reciprocal exchange of genetic information between two homologs (the nearly identical chromosomes from each parent). Alternatively, annealing can occur with the sister chromatid, which is genetically identical and cannot form a genetic

recombinant (reviewed in Kuo et al. 2021). Gene conversion, which represents a unidirectional transfer of genetic information from one homolog to the other, is often associated with a CO, the reciprocal exchange of flanking DNA between homologs (reviewed in Berchowitz and Copenhaver, 2010). Gene conversion with or without a crossover (non-CO) can occur between homologous chromosomes. For most organisms, at least one CO is formed per chromosome pair to ensure correct segregation of the chromosomes during anaphase I (Mercier et al. 2015). However, exceptions have been reported; male *Drosophila melanogaster* and female *Bombyx mori* lack COs with no apparent defect in chromosome segregation (Morgan, 1910; Rasmussen, 1977).

Early cytological investigations of meiotic chromosomes revealed several distinct features between somatic and meiotic cells. The duration of meiotic S-phase appears to be significantly longer in several plant and mammalian species (2-6-fold depending on the species) compared to mitotic S-phase (Bennett and Smith, 1972; Callan, 1973; Cha et al. 2000; Holm, 1977). A longer duration of meiotic S-phase was also reported in *Mus musculus* using genomic approaches, and a reduction in replication origin firing was suggested as the cause of this delay (Pratto et al., 2021). Moreover, the volume of chromatin and the nuclear size are larger in meiocytes (Figure 1A-B), and meiotic chromosomes adopt a dense linear structure not observed with somatic chromosomes (Figure 1C-D) (Bennett and Smith, 1972). In *Saccharomyces cerevisiae* and *Schizosaccharomyces pombe*, Spo11, the protein forming meiotic DSBs, and the cohesin subunit Rec8, become associated with chromosomes at pre-meiotic G1 and S-phases (Cha et al., 2000; Kugou et al., 2009; Watanabe et al., 2001). In these species, DNA replication is synchronised with the recruitment of meiotic proteins and is under the control of cell cycle regulatory kinases (Cdc7 in *S. cerevisiae*) (Murakami and Keeney, 2014). In the absence of *S. cerevisiae* Spo11, the duration of meiotic S-phase is decreased while the absence of Rec8 causes an increase in S-phase period (Cha et al., 2000). The coordination between DNA replication and the recruitment of meiotic proteins is a prerequisite for recombination and chromosomal processes taking place during meiosis. For

instance, the pattern of meiotic recombination correlates with the pattern of germline replication in *M. musculus* and humans (Pratto et al., 2021), and meiosis initiated without a pre-meiotic S-phase exhibits recombination defects and a mitotic-like chromosome segregation pattern in *S. pombe* (Watanabe et al., 2001).

Following DNA replication, the chromatin expands along a dense linear structure, as observed under an electron microscope, and described as the chromosome axis (Figure 1D) (Kleckner et al., 2004). The composition of the chromosome axis appears to be highly conserved between species and is composed of cohesin, coiled-coil proteins such as *S. cerevisiae* Red1, and HORMA (in reference to **Ho**p1, **R**ev7 and **MA**D2)-domain-containing proteins (Table 1). Genes coding for coiled-coil and HORMA-domain-containing axis proteins (HORMADs) are expressed specifically during meiosis (Figure 1E).

Cohesin is a multi-subunit complex with a ring structure essential to entrap DNA. The cohesin ring moves along the entrapped DNA to form a chromatin loop through a loop extrusion mechanism (reviewed in Davidson and Peters, 2021). The cohesin ring is composed of two Structural Maintenance of Chromosome (SMC) proteins, one kleisin and one stromal antigen (SA) protein (reviewed in Ishiguro, 2019). The SMC proteins are mostly conserved across species, expressed ubiquitously, and consist of SMC1 and SMC3 in *Arabidopsis thaliana*, *S. cerevisiae* and *D. melanogaster*; Psm1 and Psm3 in *S. pombe*; and SMC-1 and SMC-3 in *Caenorhabditis elegans*. In *M. musculus*, three SMC proteins are expressed: SMC1α, SMC1β and SMC3, among which only SMC1β is expressed specifically during meiosis (reviewed in Ishiguro, 2019). Plants and yeasts express the meiosis specific kleisin Rec8. *C. elegans* has 3 meiotic kleisin proteins; COH-3, COH-4 and REC-8. COH-3 and COH-4 are functionally redundant and have functions distinct from those of REC-8. For instance, sister chromatin cohesion is more severely affected in *rec*-8 than in *coh-3 coh4,* and *rec-8 coh-3 coh4* triple mutant has almost no sister chromatin cohesion (Crawley et al., 2016). *M. musculus* has three kleisins, with Rad21 being ubiquitously expressed, whereas Rad21L and Rec8 are meiosis-specific with a role in chromosome axis formation (Ward et al., 2016). In contrast, *D.*

melanogaster has two functionally distinct cohesin complexes; SOLO and the SA protein called SUNN are required for sister-chromatid cohesion, and the klesisn C(2)M and Stromalin are required for homolog interactions (Gyuricza et al. 2016). In contrast, *A. thaliana* and *S. cerevisiae* express only one meiotic SA protein called SCC3. *S. pombe* has two SA proteins Psc3 and Rec11, and only Rec11 is meiosis specific. Similarly, *M. musculus* has SA1, SA2 and SA3 (also called STAG3), with only SA3 being meiosis specific (reviewed in Ishiguro, 2019). These observations are representative of the similarities and differences of meiotic proteins and events among species, perhaps a reflection of the rapid evolution of meiosis.

Meiotic cohesin has a major role in organising the chromatin in loop arrays along the chromosome axis (Figure 1E) (Lambing et al., 2020b; Schalbetter et al., 2019). The role of cohesin is tightly regulated and is under the control of WAPL and PDS5. These two cohesin regulators are expressed in mitotic and meiotic cells and influence the association of cohesin with DNA to control chromatin organisation. In *S. pombe* and *S. cerevisiae,* chromatin compaction is reduced in *rec8* mutants, whereas the chromosome axes are shortened and the chromatin is more compact in either *pds5* or *wapl* mutants (Challa et al., 2016; Ding et al., 2016, Jin et al., 2009; Schalbetter et al., 2019). In *C. elegans wapl-1* mutant, COH-3 and COH-4, but not REC-8, accumulate on meiotic chromosomes, the chromosomes appear more compact, and the chromosome axis is shorter (Crawley et al., 2016). Intriguingly, the loss of Wapl in *M. musculus* leads to the accumulation of cohesin on the chromosomes and the formation of a dense meiotic-like axis structure in embryonic fibroblasts, revealing the propensity of somatic cohesin to form a dense chromosome axis in a deregulated environment (Tedeschi et al., 2013).

Meiotic recombination also influences chromatin interaction and the structure of the chromosome axis. The annealing of ssDNAs to the homologous chromosomes promotes novel chromatin interactions (Schalbetter et al., 2019; Zuo et al., 2021). In addition, homologous recombination facilitates the juxtaposition of homologous chromosomes leading to the formation of the synaptonemal complex (SC) in most studied organisms, with a few

exceptions. For instance, *S. pombe* has an axial structure lacking all components of the central regions of the SC, while *C. elegans* and female *D. melanogaster* form a SC independently of meiotic recombination (reviewed in Zickler and Kleckner, 1999). The SC has an evolutionarily conserved tripartite proteinaceous structure composed of two lateral elements, derived from axes of two homologous chromosomes, positioned in parallel orientation to each other and connected by transverse filaments located in the central region (Figure 2).

2. Evolution of the core axis proteins and the synaptonemal complex.

HORMADs and coiled-coil proteins belong to two protein families with structural domains that are conserved across species (Figure 3). HORMADs are involved in several key meiotic processes, such as the formation of DSBs (function not conserved across all orthologs) and COs (function conserved across all orthologs) (Table 1). All HORMADs contain a short charged-hydrophobic amino acid patch called a closure motif. This closure motif allows HORMADs to undergo conformational changes between a closed and an unlocked state. These conformational changes influence protein interactions and the assembly and disassembly of the HORMADs on chromosomes, which is necessary for meiotic recombination and synapsis (West et al., 2018; Yang et al., 2020a, Yang et al., 2020b). Hop1/ASY1/HORMAD2 interacts with the HORMA-binding closure motifs of Red1/ASY3/SYCP2 and this interaction is necessary for their recruitment to the chromosome axis (West et al., 2019). The mode of recruitment of HORMADs to the chromosomes appears to be linked to the conserved core axis proteins in these species.

However, separation of function between HORMADs is apparent in some species. For instance, *A. thaliana ASY1* is highly expressed in meiosis and promotes CO formation, while *ASY2* shows limited expression; no functional redundancy has been reported between the two HORMADs (Table 1). A separation of function between *M. musculus* HORMAD1 and HORMAD2 in meiotic recombination has also been reported and HORMAD1 appears to have

a dominant role in this process (Shin et al., 2010; Wojtasz et al., 2012) (Table 1). Hop1, ASY1 and HORMAD1 all share the common HORMA domain, but as these proteins evolved from yeast to humans, the proteins became smaller in size. *S. cerevisiae* Hop1 has 605 amino acids and *A. thaliana* ASY1 has 596 amino acid; these proteins are approximately 1.5 times longer than HORMAD1 in humans. In addition to the HORMA domain, the *S. cerevisiae* Hop1 protein contains a zinc finger motif, and this domain is replaced by a SWIRM domain in *A. thaliana* ASY1 protein. In contrast, HORMAD1 contains only the HORMA domain (Figure 3). Both the zinc finger and SWIRM domains can bind DNA and might play a role in how Hop1 and ASY1 are loaded onto chromosomes. Although HORMAD1 lacks the DNA binding element, a recent study showed that meiotic cohesins REC8 and RAD21L mediate initial loading of HORMAD1 to the chromosomes (Fujiwara et al., 2020).

In the yeast *Zygosaccharomyces rouxii*, the coiled-coil axis protein Red1 contains a 7 amino acid peptide stretch towards the C-terminal coiled-coil end that is responsible for axis formation (West et al., 2019). This property of the coiled-coil axis proteins to form an axis is conserved in mammals and plants. But as organisms evolve, the roles of axis formation and protein tetramerization become more distinct and evolve as separate protein functions. For example, in mammals, the SYCP2:SYCP3 antiparallel hetero-tetramer conformation is preferred over a homo-tetramer allowing for axis formation and bundling which leads to a stable core axis (West et al., 2019). In plants, ASY3 and ASY4 are orthologs of SYCP2 and SYCP3 and their functions are predicted to be conserved based on yeast two-hybrid interactions studies (West et al., 2019). Thus, the oligomerization and DNA interaction of axis proteins appears to be a crucial and evolutionarily conserved aspect of core axis formation.

3. Morphogenesis and remodelling of the chromosome axis

The chromosome axis results from a hierarchical assembly of the different axis proteins (Figure 2). As noted above, the loading of cohesin on the chromosomes is a prerequisite for the recruitment of the other axis components (coiled-coil and HORMADs) (Fujiwara et al., 2020; Lambing et al., 2020b; Severson et al., 2009; Sun et al., 2015). In the absence of Rec8, shorter, and sometimes fatter, axis-like structures or aggregates of axis proteins (polycomplexes) are formed in plants, yeasts, *M. musculus* and *C. elegans*. These aberrant structures often contain cohesin, coiled-coil proteins and HORMADs, such as in *M. musculus* and *A. thaliana* (Ward et al., 2016 Lambing et al., 2020b). Red1/ASY3 forms the second factor, after cohesin, to orchestrate axis morphogenesis, as it is required for the association of Hop1 with the chromosomes. In contrast, the role of Hop1/ASY1 in the recruitment of axis proteins is limited and varies between species. In *S. cerevisiae*, Hop1 modulates the distribution of Red1 genome-wide only when Rec8 is absent (Sun et al., 2015), while the localisation of *S. pombe* Rec10 (Red1 ortholog) at DSB hotspots is dependent on Hop1 (Kariyazono et al., 2019). As opposed to *S. cerevisiae*, the localisation of *A. thaliana* ASY3 (Red1 ortholog) does not require ASY1 (Hop1 ortholog) (Ferdous et al., 2012).

In *C. elegans*, no coiled-coil protein has been found associated with the chromosome axis. However, four HORMADs were identified, and their localisations are also hierarchical. All four HORMADs are dependent on the presence of the cohesin subunits COH-3, COH-4 and REC-8 (Severson et al., 2009). Following the loading of cohesin, HTP-3 is essential to recruit the other three HORMADs HTP-1, HTP-2 and HIM-3. Super-resolution imaging of meiotic chromosomes stained for axis proteins showed that HORMADs are located in the inner part while cohesins are located in the outer part of the lateral element in *C. elegans* (Figure 2) (Köhler et al., 2017).

During chromosome pairing and the establishment of the SC, the chromosome axis is remodelled and HORMADs are dissociated from the axis by Pch2/Trip13 in *S. cerevisiae, A. thaliana* and *M. musculus* (Börner et al., 2008; Lambing et al., 2015; Roig et al., 2010). Co-localisation studies of Zip1/ZYP1/SYCP1 and Hop1/ASY1/HORMAD1/HORMAD2 suggest

that the two proteins are mostly not co-localised in wild type conditions but show overlapping signal in *pch2/Trip13* mutants (Börner et al., 2008; Lambing et al., 2015; Roig et al., 2010). The exact role of the axis remodeling is not completely understood, but it is thought to be linked with the progression of meiotic recombination and the cell cycle, given the role of meiotic HORMADs in regulating cell cycle progression.

Genome-wide localisation of axis proteins is influenced by transcription and epigenetic marks in several species. For example, *S. cerevisiae* Rec8 is enriched in the intergenic regions between convergent genes that are actively transcribed (Sun et al., 2015). Since Rec8 is a prerequisite for recruiting the other axis proteins on the DNA, a similar enrichment toward the 3' end of convergent genes was also observed for Red1 (Sun et al., 2015). This pattern appears to be conserved between species, as *A. thaliana* REC8 occupancy is low and polarised toward the 3' end of transcribed genes and transposons (Lambing et al., 2020b). In *S. pombe*, the pericentromeres are mostly composed of transposons that are transcriptionally repressed by chromatin marks and H3K9 methylation; the chromodomain protein Swi6 and the histone methyltransferase Clr4 are required for the recruitment of Rec8 to the pericentromeric regions (Kitajima et al., 2003; Nambiar and Smith, 2018). Swi6 has an additional role in meiosis as it prevents the recruitment of Rec11 cohesin subunit (Scc3 or STAG3 ortholog) at the pericentromeric regions to repress the formation of meiotic DSBs near centromeres (Nambiar and Smith, 2018). The *A. thaliana* genome contains an even larger region of heterochromatin compared to *S. pombe*. The loss of H3K9me2 in *A. thaliana suvh4 suvh5 suvh6* triple mutants is associated with a redistribution of REC8 over the pericentromeric regions. Certain transposons that become transcriptionally upregulated are associated with a reduction of REC8 occupancy, revealing a link between histone modification, transcription and REC8 localisation (Lambing et al., 2020b). It is likely that other histone modifications influence the morphology of the axis. In *S. cerevisiae*, Esa1 is the catalytic subunit of the NuA4 complex and is responsible for histone acetylation. Esa1 regulates the length of the chromosome axis and the degree of chromosome compaction, and this is

associated with a significant reduction in the level of histone acetylation during meiosis (Wang et al., 2021).

4. Roles of chromosomal axis proteins in DSB and crossover formation during meiosis

CO formation during meiosis appears to stem from DSB formation in all species examined. In the few species examined, DSBs are not uniformly distributed: in yeasts and *M. musculus*, they do not appear in regions with few or no COs, such as pericentric regions, and they appear at high frequency at special sites, called DSB hotspots, scattered across the rest of the genome (Cromie et al., 2007; Gerton et al., 2000; Lange et al., 2016). Where tested, DSB hotspots are also hotspots of gene conversion or crossing over or both (e.g., Cromie et al., 2005). In *A. thaliana* and *Zea mays*, DSBs arise in regions even with low CO rates, such as the pericentric regions (Choi et al., 2018; He et al., 2017); presumably these DSBs are repaired as gene conversion or by repair with the sister chromatid (Shi et al., 2010), as discussed below.

Spo11 strictly requires several partner proteins for DSB formation (Keeney, 2007). Other proteins, such as those of the axis (Table 1), stimulate Spo11 activity or enhance Spo11's binding to the chromosome, sometimes in a region- or hotspot-specific manner. For example, the *S. cerevisiae* axis proteins Red1 and Hop1 are required nearly genome-wide for wild-type levels of DSB formation (Lam, 2016). These axis proteins recruit the DSB-forming complex or part of it. *S. cerevisiae* Hop1 binds to Mer2, an essential partner of the Spo11 complex (Panizza et al., 2011; Rousová et al., 2021). Similar interactions occur between HORMADs and Mer2 orthologs Rec15 in *S. pombe,* IHO1 in *M. musculus* and PRD3 in *A. thaliana* (Kariyazono et al., 2019; Stanzione et al., 2016; Vrielynck et al., 2021). The recruitment of Mer2 and its orthologs to the axis appears conserved across species; PRD3 foci are reduced

in *asy1* and *asy3* (Vrielynck et al., 2021), and axis-bound IHO1 localisation is reduced in *Sycp2* (Fujiwara et al., 2020).

Hop1 is required for some but not all DSB formation in *S. cerevisiae* and *S. pombe* (Kariyazono et al., 2019; Schwacha and Kleckner, 1994), but its ortholog ASY1 is not required in *A. thaliana* (Ferdous et al. 2012). The assembly of the pre-DSB complex diverges between *S. cerevisiae* and *A. thaliana.* In *S. cerevisiae,* Mer2 physically interacts with the two DSB factors Rec114 and Mei4, whereas no interaction between PRD3 and PHS1 (Rec114 ortholog) or PRD2 (Mei4 ortholog) was detected in *A. thaliana* (Vrielynck et al., 2021). The non-canonical assembly of *A. thaliana* pre-DSB complex may relate to the lack of DSB defect in *asy1.*

S. pombe Rec10, which has limited homology with Red1, also binds Rec15 (Kariyazono et al., 2019) and is required for essentially all DSBs across the genome (Fowler et al., 2013). Three small linear element proteins with which Rec10 co-localizes (Rec25, Rec27, and Mug20) are required for DSBs at most but not all hotspots (Fowler et al., 2013). The three small proteins also bind to hotspot sites, even in Rec12's absence, with high specificity and thus are protein determinants of DSB hotspots nearly genome-wide (Fowler et al., 2013). Histone modification, such as trimethylation of histone H3, is associated with hotspot formation in *S. cerevisiae* and *M. musculus* (Borde et al., 2009; Baudat et al., 2010; Parvanov et al. 2010). In *S. cerevisiae,* Mer2 interacts with Spp1, a histone H3K4 methyltransferase, and it was proposed that this interaction promotes DSB formation by tethering the region of a chromatin loop containing H3K4me3 with the chromosome axis (Sommermeyer et al., 2013). Other identified proteins, including several transcription factors, are hotspot determinants but at a more limited set of sites (*e.g.*, Mieczkowski et al., 2006). The meiosis-specific cohesin subunit Rec8 is strongly required for DSB formation at most hotspots in *S. pombe* (Fowler et al., 2013) but is required to a lesser extent, in a region-specific manner, in *S. cerevisiae* (Kugou et al., 2009). In the mutants mentioned here, COs and DSBs are reduced co-ordinately, except that in *A. thaliana* using cytological assays, COs, but not DSBs, are reduced in *asy1* mutants, although they are

both reduced in *rec8* and *asy3* mutants (Table 1) (Ferdous et al. 2012; Lambing et al., 2020b). Thus, some feature in addition to DSB frequency can govern CO frequency.

DSB repair with the homolog can produce a CO, a gene conversion, or both, but repair can also occur with the sister chromatid and produce (usually) no genetic recombinant, since the sisters are genetically identical. The choice of DNA for DSB repair is controlled in part by axis proteins and DNA strand-exchange proteins (see review by Humphryes and Hochwagen, 2014). Partner choice is most rigorously assayed as the relative frequency of intersister (IS) and interhomolog (IH) DNA joint molecules (Holliday junctions, or HJs). In *S. cerevisiae* the HJ assay has most frequently used the artificial *HIS4-LEU2* hotspot, which has insertions of *LEU2* and bacterial DNA into the *HIS4* locus. This assay shows that the axis proteins Red1 and Hop1; the cohesin subunit Rec8; and the strand-exchange proteins Dmc1 (meiosis-specific) and Rad51 affect the IS:IH ratio. For example, the IS:IH HJ ratio is about 1:5 in wild-type *S. cerevisiae* cells, 1:1 in *rec8Δ*, and 10:1 in *red1Δ* mutants (Kim et al., 2010). In *S. cerevisiae,* phosphorylation of Hop1 by Tel1 and Mec1 (homologs of ATM and ATR DNA damage response protein kinases) has been implicated in partner choice (Carballo et al., 2008). The partner choice differs among DSB hotspots and between species. Indeed, at *S. pombe ade6* DSB hotspots, the IS:IH ratio ranges from ~6:1 with an array of *lacO* operator sequences activated by a Mug20-LacI fusion to ~3:1 with the native *mbs1* hotspot and the Atf1-Pcr1-activated hotspot *ade6-3049* (Hyppa et al., 2021). Thus, axis proteins appear to have an important role in partner choice for DSB repair and recombination (Table 1).

The mechanism of partner choice for DSB repair is still unclear. One view, based on observations in *S. cerevisiae*, is that meiotic DSB repair is intrinsically with the homolog, but Rec8 cohesin switches repair to the sister; Red1 and Hop1, acting with strand exchange proteins Rad51 and Dmc1, counteracts Rec8, returning repair to the homolog in meiosis (Kim et al., 2010). Further research may reveal additional roles for axis proteins and other factors involved in partner choice, which is critical for successful meiosis.

5. Does the chromosome axis play a role in CO interference?

CO interference describes the enigmatic phenomenon that when one CO forms at a particular chromosomal location it reduces the likelihood of additional COs forming nearby, influencing the eventual spacing and number of COs along individual chromosomes (Figure 4A). Despite interference being studied for over a century (Sturtevant, 1915), the functional role of the meiotic axis in mediating interference is still hotly debated.

Several mechanistic models have been proposed to explain interference (reviewed in: Chuang and Smith, this issue; Otto and Payseur, 2019) with some early models postulating that interference is mediated by assembly of, or transmission via, the SC (Egel, 1995). However, later studies questioned the role of the SC in interference. In *S. cerevisiae,* genetic interference is abolished in *zip1* mutants, which lack an SC (Sym and Roeder, 1994), but synapsis initiation complexes (SICs), which assemble in advance of the SC, maintain CO-like interference when assayed cytologically (Fung et al., 2004). This suggests that cytological interference is, at least in part, independent of the SC. *Sordaria* SICs also display cytological interference (Zhang et al., 2014a). Additionally, in *D. melanogaster* (Page and Hawley, 2001), a *c(3)G* mutant exhibits defective SC assembly but retains genetic interference.

The axis, which forms before SC assembly, then entered the spotlight as a prime candidate for transmitting interference. In support of this, perturbations of the axis can exert measurable effects on interference in a variety of organisms. For example, interference is abrogated in mutants of the HORMADs HIM-3 (Nabeshima et al., 2004) and ASY1 (Lambing et al., 2020a) in *C. elegans* and *A. thaliana*, respectively. ASY1 (along with other axis and SC proteins) is also under strong selection in the model autotetraploid plant species *Arabidopsis arenosa* (Hollister et al., 2012), in which interference has evolved to stabilize polyploid meiosis (Morgan et al., 2021b). By genetic analyses, interference is defective in *pch2* null-mutants in both *S. cerevisiae* and *A. thaliana* (Joshi et al., 2009, Lambing et al. 2015). However, neither of these

mutants affects interference assayed cytologically (Lambing et al. 2015; Zhang et al., 2014c). In *S. cerevisiae*, mutation of SUMOylation sites in axis proteins TopoII and Red1 weakens interference by cytological assay (Zhang et al., 2014c).

The reliance of interference in *S. cerevisiae* on the catalytic activity of TopoII lends support to a mechanical 'stress and stress relief' model for interference (Kleckner et al., 2004), where interference is transmitted by the accumulation, relief and redistribution of mechanical stress along the meiotic axis. A mathematical model (the 'beam-film' model) has also been formulated to quantitatively describe this mechanical process and has been successfully used to explain various aspects of CO patterning in several organisms (Zhang et al., 2014b).

Despite this, a potential role for the SC, rather than the axis, in mediating interference has experienced a revival in recent years. In *A. thaliana* and *S. cerevisiae*, both synapsis and genetic interference are abolished in mutants lacking the SC transverse filament protein ZYP1 or ZIP1, whilst axis formation appears uncompromised (Capilla-Pérez et al., 2021; France et al., 2021; Sym and Roeder, 1994). In *C. elegans*, the liquid crystalline SC functions to spatially compartmentalise recombination proteins along paired chromosomes (Rog et al., 2017), and partial depletion of SC protein SYP-1 impairs interference (Libuda et al., 2013). In some species that either lack or exhibit only weak interference, such as the fungi *S. pombe* and *Aspergillus nidulans,* the SC is conspicuously absent (reviewed in: Chuang and Smith, this issue; Zickler and Kleckner, 1999). Whilst *S. pombe* also lacks other ZMM proteins, such as the E3 ligase Zip3, the protist *Tetrahymena* lacks an SC and still requires Zip3 orthologues for CO formation (Shodhan et al., 2017). However, it remains unclear if *Tetrahymena* COs exhibit interference (Loidl, 2021).

The synthesis of these findings, combined with knowledge that interference strength is dependent upon the dosage of the Zip3 orthologue HEI10 in *A. thaliana* (Ziolkowski et al., 2017), has contributed to the development of an alternative 'coarsening' model for interference. Here, CO patterning and interference are driven by the competitive coarsening of HEI10 protein clusters along pachytene bivalents (Morgan et al., 2021a). This model is

supported experimentally by quantitative cytological observations of HEI10 protein clusters and predictive mathematical simulations (Figure 4B-D). As HEI10 is a member of a conserved family of RING-finger proteins with similar meiotic function, this coarsening paradigm may represent a conserved process explaining CO positioning in diverse species, although this has yet to be explicitly demonstrated. Thus, determining whether the axis plays a direct role (e.g., by modulating the coarsening dynamics of HEI10 or transmitting physical tension) or indirect role (e.g. by coordinating synapsis or determining bivalent length) in the mechanism of interference remains an exciting avenue for future study.

6. Temperature-based regulation of axis proteins and the impact on recombination

Fluctuations in temperature are known to affect recombination rates and patterns (reviewed in Morgan et al., 2017). Using electron microscopy and immunofluorescence, it has also been observed in various species that elevated temperatures can cause aggregation of the normally linear meiotic axis and the formation of SC polycomplexes (Figure 5A-B) (Morgan et al., 2017). For example, in *A. thaliana* at 20°C the axis proteins ASY1, ASY4, REC8, and the SC protein ZYP1, assemble linearly during prophase I, while at an elevated temperature of 37°C the assembly of ASY1, ASY3 and ZYP1 (but not REC8) is disrupted and the proteins appear as punctate foci (Fu et al., 2021; Ning et al., 2021). Similar observations were also made for ASY1 and ZYP1 in *A. arenosa* grown at 22°C and 33°C (Morgan et al., 2017) (Figure 3A) and, intriguingly, axis and SC proteins also appear to have undergone selection in *A. arenosa* populations adapted to warmer climates (Wright et al., 2015). In *A. thaliana*, heat-stress also affects meiotic DSB number (Ning et al., 2021), chromosomal segregation (de Storme and Geelen, 2020), meiotic duration (de Jaeger-Braet et al., 2021) and the expression of numerous meiotic genes (Huang et al., 2021). For example, in *A. thaliana*, as well as *Hordeum vulgare*,

ASY1 expression is upregulated at high temperatures of 28°C and 30°C, respectively (Huang et al., 2021; Oshino et al., 2007).

With the advent of protein structure prediction, it is now possible to assess predicted structural elements of axis and SC proteins across kingdoms. In these predicted structures, several axis proteins contain intrinsically disordered regions which act as linkers between structured domains. For example, the predicted structure of the core axis proteins Red1 and Rec10 from *S. cerevisiae* and *S. pombe*, respectively, shows this feature, as do its plant (ASY3) and mammalian orthologs (SYCP2) (Figure 5B). They all contain a coiled-coil domain which is surrounded by intrinsically disordered regions which are known to facilitate liquid-liquid phase separation to form bimolecular condensates. Furthermore, computational and experimental models show that temperature can be an important factor for driving liquid-liquid phase separation in disordered proteins (Dignon et al., 2019). Intrinsically disordered regions in *C. elegans* axis and SC proteins are also enriched in charge-interacting elements (Liu et al., 2021; Zhang et al., 2020), and mutations in these elements of SC proteins SYP-5 and SYP-4 lead to embryonic lethality at high temperature (Liu et al., 2021). Additionally, coiled-coil domains facilitate protein insolubility and aggregation at varying temperatures (Fiumara et al., 2010) and are dominant structural elements of SC transverse filament proteins (Zip1 in *S. cerevisiae*, ZYP1a and ZYP1b in *A. thaliana*, and SYCP1 in *M. musculus*).

Structural studies are, therefore, essential for uncovering how and why individual meiotic proteins and protein complexes are affected by temperature and combining these with molecular and cell biology approaches will be crucial for determining the underlying causes and consequences of meiotic thermal sensitivity.

7. Aberrant expression of the HORMADs and SC proteins regulates intrinsic DNA repair activities in somatic cancer cells

Although the SC proteins and HORMADs have long been considered to be expressed only in the germ cells, accumulating evidence has shown that these meiotic proteins are also aberrantly expressed in various somatic human cancer cells (Hosoya and Miyagawa, 2021a; Simpson et al., 2005). Such proteins have been called “the cancer/testis antigens” from their unique expression patterns and have been considered to be promising targets for cancer immunotherapy. Recently, the SC proteins SYCP3 and SYCE2, and the HORMAD1 protein, have been reported to regulate intrinsic DSB repair activities in cancer, suggesting the roles of these proteins in the maintenance of genome integrity in somatic cells (Gao et al., 2018; Hosoya et al., 2012; Hosoya et al., 2018; Nichols et al., 2018).

SYCP3 is a component of the axial and lateral elements of the SC in meiotic cells. In somatic cells, SYCP3 expression has been documented in various cancers (Hosoya and Miyagawa, 2021a) and can be induced in SYCP3-nonexpressing cancer cells by treatment with the demethylating agent 5-azacytidine, indicating that a demethylation-dependent process is responsible for its ectopic expression (Hosoya et al., 2012). Clinical studies reveal that SYCP3 expression level may serve as a prognostic predictor for poor overall survival in cervical cancer and non-small cell lung cancer (Cho et al., 2014; Chung et al., 2013; Kitano et al., 2017). Mechanistically, SYCP3 inhibits intrinsic homologous recombination (HR) repair pathway for DSBs by interacting with BRCA2, a tumor suppressor whose mutations are responsible for hereditary breast and ovarian cancers (Hosoya et al., 2012). While BRCA2 binds to the meiosis-specific proteins MEILB2 and BRME1 and mediates strand invasion by RAD51 and DMC1 in meiotic recombination (Takemoto et al., 2020; Zhang et al., 2020), BRCA2 plays a mediator role at the early stages of HR by directly binding to RAD51 during mitotic recombination. MEILB2 and BRME1 are also found activated in certain human cancers (Zhang et al., 2020). This inhibitory effect of SYCP3 on intrinsic HR in somatic cells is not only important as a cause of genomic instability but also provides an important clue in developing a novel therapeutic strategy for cancer. Cancer cells defective in HR are hypersensitive to poly(ADP-ribose) polymerase (PARP) inhibitors based on the principle of synthetic lethality,

where the single-strand break repair pathway that compensates for the defects of HR in cancer cells is disrupted, leading to cancer-specific cell death (Hosoya and Miyagawa, 2014). While this concept is now being applied to BRCA1- or BRCA2-mutated cancers in cancer precision medicine (Hosoya and Miyagawa, 2021b), SYCP3-expressing cancers may also be sensitive to PARP inhibitors, even if they do not have BRCA mutations, which remains to be elucidated in the future.

SYCE2 is a component of the central elements of the SC in meiotic cells. It is also expressed at varying levels in somatic cancer cells, and its expression can be epigenetically induced by treatment with 5-azacytidine, like SYCP3 (Hosoya et al., 2018). Mechanistically, SYCE2 directly binds to heterochromatin-related protein HP1α through its N-terminal hydrophobic sequence and dissociates HP1α from trimethylated histone H3 lysine 9 (H3K9me3) to potentiate ATM-mediated DSB repair activity even in the absence of exogenous DNA damage (Hosoya et al., 2018). Among the DSB repair pathways, both HR and non-homologous end joining (NHEJ) are activated by SYCE2. These findings suggest that SYCE2 plays a role in the link between the nuclear microenvironment and the DNA damage response and repair when ectopically expressed in somatic cancer cells.

HORMAD1 expression is also observed in various cancers (Chen et al., 2005) and can be induced by treatment with 5-azacytidine (Nichols et al. 2018), like SYCP3 and SYCE2. Recent reports suggest that HORMAD1 promotes HR (Gao et al., 2018; Nichols et al., 2018). One report showed that generation of RPA foci, a protein binding to single-stranded DNA, was reduced by HORMAD1 depletion, suggesting that HORMAD1 promotes DSB end resection (Gao et al., 2018), whereas another report showed that HORMAD1 promoted RAD51-filament formation but not DNA resection (Nichols et al., 2018). Thus, the exact mechanisms and direct targets through which HORMAD1 regulates HR remain to be addressed. HORMAD1 expression in cancer cells correlates with resistance to DNA-damaging agents or PARP inhibitors (Nichols et al., 2018; Shahzad et al., 2013; Wang et al., 2018), in accord with the HR-promoting effect of HORMAD1.

These recent findings highlight the significance of meiosis-specific proteins in cancer biology and have great potential to impact the development of novel targeted cancer therapy. Thus, it would be worth investigating the currently unrecognized somatic roles of meiosis-related cancer/testis antigens to improve our understanding in mechanisms for cancer development and targets for cancer therapy.

References

Anderson, L.K., Royer, S.M., Page, S.L., McKim, K.S., Lai, A., Lilly, M.A., Hawley, R.S. (2005). Juxtaposition of C(2)M and the transverse filament protein C(3)G within the central region of Drosophila synaptonemal complex. *Proc Natl Acad Sci USA. 102*: 4482-4487.

Barakate, A., Orr, J., Schreiber, M., Colas, I., Lewandowska, D., McCallum, N., Macaulay, M., Morris, J., Arrieta, M., Hedley, P.E., Ramsay, L., Waugh, R. (2021). Barley anther and meiocyte transcriptome dynamics in meiotic prophase I. *Front Plant Sci. 11*: 619404.

Baudat, F., Buard, J., Grey, C., Fledel-Alon, A., Ober, C., Przeworski, M., Coop, G., de Massy, B., (2010). PRDM9 is a major determinant of meiotic recombination hotspots in humans and mice. *Science. 327:* 836-840.

Bennett, M.D., Smith, J.B. (1972). The effect of polyploidy on meiotic duration and pollen development in cereal anthers. *Proc R Soc Lond. 181*: 81-107.

Berchowitz, L.E., Copenhaver, G.P. (2010). Genetic interference: don't stand so close to me. *Curr Genomics. 11:* 91-102.

Bhattacharyya, T., Walker, M., Powers, N.R., Brunton, C., Fine, A.D., Petkov, P.M., Handel, M.A. (2019). Prdm9 and meiotic cohesin proteins cooperatively promote DNA double-strand break formation in mammalian spermatocytes. *Curr Biol. 29*: 1002-1018.

Boden, S.A., Langridge, P., Spangenberg, G., Able, J.A. (2009). TaASY1 promotes homologous chromosome interactions and is affected by deletion of *Ph1. Plant J. 57*: 487-97.

Borde, V., Robine, N., Lin, W., Bonfils, S., Géli, V., Nicolas, A. (2009). Histone H3 lysine 4 trimethylation marks meiotic recombination initiation sites. *EMBO J. 28:* 99-111.

Börner, G.V., Barot, A., Kleckner, N. (2009). Yeast Pch2 promotes domanial axis organization, timely recombination progression, and arrest of defective recombinosomes during meiosis. *Proc Natl Acad Sci USA. 105*: 3327-32.

Brar, G.A., Yassour, M., Friedman, N., Regev, A., Ingolia, N.T., Weissman, J.S. (2012). High-resolution view of the yeast meiotic program revealed by ribosome profiling. *Science. 335*: 552-557.

Cahoon, C.K., Yu, Z., Wang, Y., Guo, F., Unruh, J.R., Slaughter, B.D., Hawley, R.S. (2017). Superresolution expansion microscopy reveals the three-dimensional organization of the *Drosophila* synaptonemal complex. *Proc Natl Acad Sci USA. 114*: E6857-6866.

Callan, H.G. (1973). DNA replication in the chromosome of eukaryotes. *Cold Spring Harbor Symp. Quant. Biol. 38*: 195-203.

Capilla-Pérez, L., Durand, S., Hurel, A., Lian, Q., Chambon, A., Taochy, C., Solier, V., Grelon, M., Mercier, R. (2021). The synaptonemal complex imposes crossover interference and heterochiasmy in Arabidopsis. *Proceedings of the National Academy of Sciences 118*: e2023613118.

Carballo, J.A., Johnson, A.L., Sedgwick, S.G., Cha, R.S. (2008). Phosphorylation of the axial element protein Hop1 by Mec1/Tel1 ensures meiotic interhomolog recombination. *Cell. 132:* 758-770.

Cha, R.S., Weiner, B.M., Keeney, S., Dekker, J., Kleckner, N. (2000). Progression of meiotic DNA replication is modulated by interchromosomal interaction proteins, negatively by Spo11p and positively by Rec8p. *Genes Dev. 14*: 493-503.

Challa, K., Lee, M-S., Shinohara, M., Kim, K.P., Shinohara, A. (2016). Rad61/Wpl1 (Wapl), a cohesin regulator, controls chromosome compaction during meiosis. *Nucleic Acids Res. 44:* 3190-3203.

Chambon, A., West, A., Vezon, D., Horlow, C., De Muyt, A., Chelysheva, L., Ronceret, A., Darbyshire, A., Osman, K., Heckmann, S., Franklin, F.C.H., Grelon, M. (2018). Identification of ASYNAPTIC4, a component of the meiotic chromosome axis. *Plant Physiol. 178*: 233-246.

Chen, Y.T., Venditti, C.A., Theiler, G., Stevenson, B.J., Iseli, C., Gure, A.O., Jongeneel, C.V., Old, L.J., Simpson A.J. (2005). Identification of CT46/HORMAD1, an immunogenic cancer/testis antigen encoding a putative meiosis-related protein. *Cancer Immun. 5*: 9.

Cho, H., Noh, K.H., Chung, J.Y., Takikita, M., Chung, E.J., Kim, B.W., Hewitt, S.M., Kim, T.W., Kim, J.H. (2014). Synaptonemal complex protein 3 is a prognostic marker in cervical cancer. *PLoS One. 9*: e98712.

Choi, K., Zhao, X., Tock, A.J., Lambing, C., Underwood, C.J., Hardcastle, T.J., Serra, H., Kim, J., Cho, H.S., Kim, J., Ziolkowski, P.A., Yelina, N.E., Hwang, I., Martienssen, R.A., Henderson, I.R. (2018). Nucleosomes and DNA methylation shape meiotic DSB frequency in *Arabidopsis thaliana* transposons and gene regulatory regions. *Genome Res 28*: 532-546.

Chung, J.Y., Kitano, H., Takikita, M., Cho, H., Noh, K.H., Kim, T.W., Ylaya, K., Hanaoka, J., Fukuoka, J., Hewitt, S.M. (2013). Synaptonemal complex protein 3 as a novel prognostic marker in early stage non-small cell lung cancer. *Hum Pathol. 44*: 472-479.

Couteau, F., Nabeshima, K., Villeneuve, A., Zetka, M. (2004). A component of C. elegans meiotic chromosome axes at the interface of homolog alignment, synapsis, nuclear reorganization, and recombination. *Curr Biol. 14*: 585-92.

Couteau, F., Zetka, M. (2005). HTP-1 coordinates synaptonemal complex assembly with homolog alignment during meiosis in C. elegans. *Genes Dev. 19*: 2744-56.

Crawley, O., Barroso, C., Testori, S., Ferrandiz, N., Silva, N., Castellano-Pozo, M., Jaso-Tamame, A.L., Martinez-Perez, E. (2016). *Elife. 5:* e10851.

Cromie, G.A., Hyppa, R.W., Cam, H.E., Farah, J.A., Grewal, S.H.I.S., and Smith, G.R. (2007). A discrete class of intergenic DNA dictates meiotic DNA break hotspots in fission yeast. *PLoS Genet. 3*: e141.

Cromie, G.A., Rubio, C.A., Hyppa R.W., Smith, G.R. (2005). A natural meiotic DNA break site in Schizosaccharomyces pombe is a hotspot of gene conversion, highly associated with crossing over. *Genetics. 169*: 595-605.

Cuacos, M., Lambing, C., Pachon-Penalba, M., Osman, K., Armstrong, S.J., Henderson, I.R., Sanchez-Moran, E., Franklin, F.C.H., Heckmann, S. (2021). Meiotic chromosome axis remodelling is critical for meiotic recombination in Brassica rapa. *J Exp Bot. 72*: 3012-3027.

Daniel, K., Lange, J., Hached, K., Fu, J., Anastassiadis, K., Roig, I., Cooke, H.J., Stewart, F.A., Wassmann, K., Jasin, M., Keeney, S., Tóth, A. (2011). Meiotic homologue alignment and its quality surveillance are controlled by mouse HORMAD1. *Nat Cell Biol. 13*: 599-610.

Davidson, I.F., Peters, J.M. (2021). Genome folding through loop extrusion by SMC complexes. *Nat Rev Mol Cell Biol. 22:* 445-464.

de Jaeger-Braet, J., Krause, L., Buchholz, A., Schnittger, A. (2021). Heat stress reveals a specialized variant of the pachytene checkpoint in meiosis of Arabidopsis thaliana. *Plant Cell.* koab257

de Storme, N., Geelen, D. (2020). High temperatures alter cross-over distribution and induce male meiotic restitution in Arabidopsis thaliana. *Communications Biology. 3*: 187.

Ding, D-Q., Matsuda, A., Okamasa, K., Nagahama, Y., Haraguchi, T., Hiraoka, Y. (2016). Meiotic cohesin-based chromosome structure is essential for homologous chromosome pairing in Schizosaccharomyces pombe. *Chromosoma. 125*: 205-14.

Dignon, G.L., Zheng, W., Kim, Y.C., Mittal, J. (2019). Temperature-Controlled Liquid–Liquid Phase Separation of Disordered Proteins. *ACS Cent Sci. 5*: 821–830.

Dukowic-Schulze, S., Sundararajan, A., Mudge, J., Ramaraj, T., Farmer, A.D., Wang, M., Sun, Q., Pillardy, J., Kianian, S., Retzel, E.F., Pawlowski, W.P., Chen, C. (2014). The transcriptome landscape of early maize meiosis. *BMC Plant Biol. 14*:118.

Ellermeier, C., Smith, G.R. (2005). Cohesins are required for meiotic DNA breakage and recombination in *Schizosaccharomyces pombe*. *Proc. Natl. Acad. Sci. USA*, *102*: 10952-10957.

Egel, R. (1995). The synaptonemal complex and the distribution of meiotic recombination events. *Trends in Genetics. 11*: 206–208.

Estreicher, A., Lorenz, A., Loidl, J. (2012). Mug20, a novel protein associated with linear elements in fission yeast meiosis. *Curr Genet*. *58*: 119-127.

Ferdous, A., Higgins, J.D., Osman, K., Lambing, C., Roitinger, E., Mechtler, K., Armstrong, S.J., Perry, R., Pradillo, M., Cunado, N., Franklin, F.C.H. (2012). Inter-homolog crossing-over and synapsis in Arabidopsis meiosis are dependent on the chromosome axis protein AtASY3. *PLoS Genet. 8*: e1002507.

Fiumara, F., Fioriti, L., Kandel, E.R., Hendrickson, W.A. (2010). Essential Role of Coiled Coils for Aggregation and Activity of Q/N-Rich Prions and PolyQ Proteins. *Cell. 143*: 1121–1135.

Fowler, K.R., Gutiérrez-Velasco, S., Martín-Castellanos, C., Smith, G.R. (2013). Protein determinants of meiotic DNA break hot spots. *Mol. Cell*. 49: 983-996.

France, M.G., Enderle, J., Röhrig, S., Puchta, H., Franklin, F.C.H., Higgins, J.D. (2021). ZYP1 is required for obligate cross-over formation and cross-over interference in Arabidopsis. *Proc Natl Acad Sci USA. 118*: e2021671118.

Fu, H., Zhao, J., Ren, Z., Yang, K., Wang, C., Zhang, Xiaohong, Elesawi, I.E., Zhang, Xianhua, Xia, J., Chen, C., Lu, P., Chen, Y., Liu, H., Yu, G., Liu, B. (2021). Interfered chromosome

pairing at high temperature promotes meiotic instability in autotetraploid Arabidopsis. *Plant Physiol kiab563*.

Fujiwara, Y., Horisawa-Takada, Y., Inoue, E., Tani, N., Shibuya, H., Fujimura, S., Kariyazono, R., Sakata, T., Ohta, K., Araki, K., Okada, Y., Ishiguro, K-I. (2020). Meiotic cohesins mediate initial loading of HORMAD1 to the chromosomes and coordinate SC formation during meiotic prophase. *PLoS Genet 16*: e1009048.

Fukuda, T., Daniel, K., Wojtasz, L., Toth, A., Höög, C. (2010). A novel mammalian HORMA domain-containing protein HORMAD1, preferentially associates with unsynapsed meiotic chromosomes. *Exp Cell Res. 316*: 158-71.

Fung, J.C., Rockmill, B., Odell, M., Roeder, G.S. (2004). Imposition of Crossover Interference through the Nonrandom Distribution of Synapsis Initiation Complexes. *Cell 116*: 795–802.

Gao, Y., Kardos, J., Yang, Y., Tamir, T.Y., Mutter-Rottmayer. E., Weissman, B., Major, M.B., Kim, W.Y., Vaziri, C. (2018). The Cancer/Testes (CT) Antigen HORMAD1 promotes Homologous Recombinational DNA Repair and Radioresistance in Lung adenocarcinoma cells. *Sci Rep. 8*: 15304.

Gerton, J.L., DeRisi, J., Shroff, R., Lichten, M., Brown, P.O., and Petes, T.D. (2000). Global mapping of meiotic recombination hotspots and coldspots in the yeast *Saccharomyces cerevisiae. Proc. Natl. Acad. Sci. USA. 97*: 11383-11390.

Goodyer, W., Kaitna, S., Couteau, F., Ward, J.D., Boulton, S.J., Zetka, M. (2008). HTP-3 links DSB formation with homolog pairing and crossing over during C. elegans meiosis. *Dev Cell. 14*: 263-74.

Gyuricza, M.R., Manheimer, K.B., Apte, V., Krishnan, B., Joyce, E.F., McKee, B.D., McKim, K.S. (2016). Dynamic and stable cohesins regulate synaptonemal complex assembly and chromosome segregation. *Curr Biol 26:* 1688-1698.

He, Y., Wang., M., Dukowic-Schulze, S., Zhou, A., Tiang, C-L., Shilo, S., Sidhu, G.K., Eichten, S., Bradbury, P., Springer, N.M., Buckler, E.S., Levy, A.A., Sun, Q., Pillardy, J., Kianian, P.M.A., Kianian, S.F., Chen, C., Pawlowski, W.P. (2017). Genomic features shaping the landscape of meiotic double-strand-break hotspots in maize. *Proc Natl Acad Sci USA. 114*: 12231-12236.

Hollister, J.D., Arnold, B.J., Svedin, E., Xue, K.S., Dilkes, B.P., Bomblies, K. (2012). Genetic Adaptation Associated with Genome-Doubling in Autotetraploid Arabidopsis arenosa. *PLoS Genetics 8*: e1003093.

Holm, P.B. (1977). The premeiotic DNA replication of euchromatin and heterochromatin in Lilium longiflorum (Thunb.). *Carlsberg Res Commun 42*: 249–281.

Hosoya, N., Miyagawa, K. (2014). Targeting DNA damage response in cancer therapy. *Cancer Sci. 105*: 370-388.

Hosoya, N., Miyagawa, K. (2021a). Synaptonemal complex proteins modulate the level of genome integrity in cancers. *Cancer Sci. 112*: 989-996.

Hosoya, N., Miyagawa, K. (2021b) Implications of the germline variants of DNA damage response genes detected by cancer precision medicine for radiological risk communication and cancer therapy decisions. *J Radiat Res. 62*: i44-i52.

Hosoya, N., Okajima, M., Kinomura, A., Fujii, Y., Hiyama, T., Sun, J., Tashiro, S., Miyagawa, K. (2012). Synaptonemal complex protein SYCP3 impairs mitotic recombination by interfering with BRCA2. *EMBO Rep. 13*: 44-51.

Hosoya, N., Ono, M., Miyagawa, K. (2018). Somatic role of SYCE2: an insulator that dissociates HP1α from H3K9me3 and potentiates DNA repair. *Life Sci Alliance*. *1*: e201800021.

Huang, J., Wang, H., Wang, Y., Copenhaver, G.P. (2021). Comparative transcriptomic analysis of thermally stressed Arabidopsis thaliana meiotic recombination mutants. *BMC genomics. 22*: 181.

Humphryes, N., Hochwagen, A. (2014). A non-sister act: recombination template choice during meiosis. *Exp Cell Res. 329*: 53-60.

Humphryes, N., Leung, W-K., Argunhan, B., Terentyev, Y., Dvorackova, M., Tsubouchi, H. (2013). The Ecm11-Gmc2 complex promotes synaptonemal complex formation through assembly of transverse filaments in budding yeast. *PLoS Genet. 9*: e1003194.

Hyppa, R.W., Cho, J.D., Nambiar, M., Smith, G.R. (2022). Redirecting meiotic DNA break hotspot determinant proteins alters localized spatial control of DNA break formation and repair. *Nucleic Acids Res. 50*: 899-914.

Ishiguro, K-I. (2019). The cohesin complex in mammalian meiosis. *Genes Cells. 24:* 6-30.

Jin, H., Guacci, V., Yu, H-G. (2009). Pds5 is required for homologue pairing and inhibits synapsis of sister chromatids during yeast meiosis. *J Cell Biol. 186:* 713-725.

Joshi, N., Barot, A., Jamison, C., Börner, G.V. (2009). Pch2 Links Chromosome Axis Remodeling at Future Crossover Sites and Crossover Distribution during Yeast Meiosis. *PLoS Genetics. 5*: e1000557.

Kariyazono, R., Oda, A., Yamada, T., Ohta, K. (2019). Conserved HORMA domain-containing protein Hop1 stabilizes interaction between proteins of meiotic DNA break hotspots and chromosome axis. *Nucleic Acids Res. 47*: 10166-10180.

Kassir, Y., Adir, N., Boger-Nadjar, E., Raviv, N.G., Rubin-Bejerano, I., Sagee, S., Shenhar, G. (2003). Transcriptional regulation of meiosis in budding yeast. *Int Rev Cytol. 224*: 111-71.

Keeney, S. (2007). Spo11 and the formation of DNA double-strand breaks in meiosis. *In recombination and meiosis: crossing-over and disjunction, R. Egel, and D.-H. Lankenau, eds. (Berlin: Springer-Verlag)*, pp. 81-123.

Kim, K.P., Weiner, B.M., Zhang, L., Jordan, A., Dekker, J., Kleckner, N. (2010). Sister cohesion and structural axis components mediate homolog bias of meiotic recombination. *Cell. 143*: 924-37.

Kitajima, T.S., Yokobayashi, S., Yamamoto, M., Watanabe, Y. (2003). Distinct cohesin complexes organize meiotic chromosome domains. *Science. 300*: 1152-5.

Kitano, H., Chung, J.Y., Noh, K.H., Lee, Y.H., Kim, T.W., Lee, S.H., Eo, S.H., Cho, H.J., Choi, C.H., Inoue, S., Hanaoka, J., Fukuoka, J., Hewitt, S.M. (2017). Synaptonemal complex protein 3 is associated with lymphangiogenesis in non-small cell lung cancer patients with lymph node metastasis. *J Transl Med*. *15*: 138.

Kleckner, N., Zickler, D., Jones, G.H., Dekker, J., Padmore, R., Henle, J., Hutchinson, J. (2004). A mechanical basis for chromosome function. *Proc Natl Acad Sci U S A. 101*: 12592-7.

Klein, F., Mahr, P., Galova, M., Buonomo, S.B., Michaelis, C., Nairz, K., Nasmyth, K. (1999). A central role for cohesins in sister chromatid cohesion, formation of axial elements, and recombination during yeast meiosis. *Cell. 98:* 91-103.

Köhler, S., Wojcik, M., Xu, K., Dernburg, A.F. (2017). Superresolution microscopy reveals the three-dimensional organization of meiotic chromosome axes in intact Caenorhabditis elegans tissue. *Proc Natl Acad Sci U S A. 114*: E4734-E4743.

Kugou, K., Fukuda, T., Yamada, S., Ito, M., Sasanuma, H., Mori, S., Katou, Y., Itoh, T., Matsumoto, K., Shibata, T., Shirahige, K., Ohta, K. (2009). Rec8 guides canonical Spo11 distribution along yeast meiotic chromosomes. *Mol Biol Cell. 20*: 3064-76.

Kuo, P., Da Ines, O., Lambing, C. (2021). Rewiring Meiosis for Crop Improvement. *Front Plant Sci. 12*: 708948.

Lam, I. (2016). The meiotic recombination initiation landscape in yeast: evolutionary dynamics and factors that shape its distribution. PhD thesis, Memorial Sloan Kettering Cancer Center.

Lambing, C., Kuo, P.C., Tock, A.J., Topp, S.D., Henderson, I.R. (2020a). ASY1 acts as a dosage-dependent antagonist of telomere-led recombination and mediates crossover interference in *Arabidopsis*. *Proc Natl Acad Sci USA. 117*: 13647-13658.

Lambing, C., Osman, K., Nuntasoontorn, K., West, A., Higgins, J.D., Copenhaver, G.P., Yang, J., Armstrong, S.J., Mechtler, K., Roitinger, E., Franklin, F.C.H. (2015). Arabidopsis PCH2 mediates chromosome remodeling and maturation of crossovers. *PLoS Genet. 11*: e1005372.

Lambing, C., Tock, A.J., Topp, S.D., Choi, K., Kuo, P.C., Zhao, X., Osman, K., Higgins, J.D., Franklin, F.C.H., Henderson, I.R. (2020b). Interacting Genomic Landscapes of REC8-Cohesin, Chromatin, and Meiotic Recombination in Arabidopsis. *Plant Cell. 32*: 1218-1239.

Lange, J., Yamada, S., Tischfield, S.E., Pan, J., Kim, S., Zhu, X., Socci, N.D., Jasin, M., Keeney, S. (2016). The Landscape of Mouse Meiotic Double-Strand Break Formation, Processing, and Repair. *Cell. 167*: 695-708.

Latypov, V., Rothenberg, M., Lorenz, A., Octobre, G., Csutak, O., Lehmann, E., Loidl, J., Kohli, J. (2010). Roles of Hop1 and Mek1 in meiotic chromosome pairing and recombination partner choice in *Schizosaccharomyces pombe*. *Mol Cell Biol. 30*: 1570-81.

Lee, D.H., Kao, Y-H., Ku, J-C., Lin, C-Y., Meeley, R., Jan, Y-S., Wang, C-J.R. (2015). The axial element protein DESYNAPTIC2 mediates meiotic double-strand break formation and synaptonemal complex assembly in maize. *Plant Cell. 27*: 2516-29.

Libuda, D.E., Uzawa, S., Meyer, B.J., Villeneuve, A.M. (2013). Meiotic chromosome structures constrain and respond to designation of crossover sites. *Nature. 502*: 703-706.

Liu, Y., Zhao, Q., Nie, H., Zhang, F., Fu, T., Zhang, Z., Qi, F., Wang, R., Zhou, J., Gao, J. (2021). SYP-5 regulates meiotic thermotolerance in Caenorhabditis elegans. *J Mol Cell Biol. 13*: 662–675.

Loidl, J. (2021). Tetrahymena meiosis: Simple yet ingenious. *PLoS Genetics. 17*: e1009627.

Lorenz, A., Estreicher, A., Kohli, J., Loidl, J. (2006). Meiotic recombination proteins localize to linear elements in *Schizosaccharomyces pombe. Chromosoma. 115*: 330-340.

Manheim, E.A., McKim, K.S. (2003). The synaptonemal complex component C(2)M regulates meiotic crossing over in Drosophila. *Curr Biol. 13*: 276-85.

Martín-Castellanos, C., Blanco, M., Rozalén, A.E., Pérez-Hidalgo, L., García, A.I., Conde, F., Mata, J., Ellermeier, C., Davis, L., San-Segundo, P., Smith, G.R., Moreno, S. (2005). A large-scale screen in S. pombe identifies seven novel genes required for critical meiotic events. *Curr Biol 15*: 2056-62

Martinez-Perez, E., Villeneuve, A.M. (2005). HTP-1 dependent constraints coordinate homolog pairing and synapsis and promote chiasma formation during C. elegans meiosis. *Genes Dev. 19*: 2727-43.

McClung, CR., Lou, P., Hermand, V., Kim, J.A. (2016). The Importance of Ambient Temperature to Growth and the Induction of Flowering. *Front Plant Sci. 7*: 1266.

McKee, B.D., Yan, R., Tsai, J-H. (2012). Meiosis in male Drosophila. *Spermatogenesis. 2*: 167-184.

Mehrotra, S., McKim, K.S. (2006). Temporal analysis of meiotic DNA double-strand break formation and repair in Drosophila females. *PLoS Genet. 2*: e200.

Mercier, R., Mezard, C., Jenczewski, E., Macaisne, N., Grelon, M. (2015). The molecular biology of meiosis in plants. *Annu Rev Plant Biol. 66:* 297-327.

Miao, C., Tang, D., Zhang, H., Wang, M., Li, Y., Tang, S., Yu, H., Gu, M., Cheng, Z. (2013). Central region component1, a novel synaptonemal complex component, is essential for meiotic recombination initiation in rice. *Plant Cell. 25*: 2998-3009.

Mieczkowski, P.A., Dominska, M., Buck, M.J., Gerton, J.L., Lieb, J.D., Petes, T.D. (2006). Global analysis of the relationship between the binding of the Bas1p transcription factor and

meiosis-specific double-strand DNA breaks in *Saccharomyces cerevisiae*. *Mol Cell Bio. 26*: 1014-1027.

Morgan, T.H. (1910). Sex limited inheritance in Drosophila. *Science 32:* 120-122.

Morgan, C., Fozard, J.A., Hartley, M., Henderson, I.R., Bomblies, K., Howard, M. (2021a). Diffusion-mediated HEI10 coarsening can explain meiotic crossover positioning in Arabidopsis. *Nat Commun. 12*: 4674.

Morgan, C., White, M.A., Franklin, F.C.H., Zickler, D., Kleckner, N., Bomblies, K. (2021b). Evolution of crossover interference enables stable autopolyploidy by ensuring pairwise partner connections in Arabidopsis arenosa. *Curr Biol. 31*: 4713-4726.

Morgan, C.H., Zhang, H., Bomblies, K. (2017). Are the effects of elevated temperature on meiotic recombination and thermotolerance linked via the axis and synaptonemal complex? *Philos Trans R Soc Lond B Biol Sci. 372*: 20160470.

Murakami, H., Keeneym S. (2014). Temporospatial coordination of meiotic DNA replication and recombination via DDK recruitment to replisomes. *Cell. 158*:861-873.

Nabeshima, K., Villeneuve, A.M., Hillers, K.J. (2004). Chromosome-Wide Regulation of Meiotic Crossover Formation in Caenorhabditis elegans Requires Properly Assembled Chromosome Axes. *Genetics. 168*:1275-92.

Nambiar, M., Smith, G.R. (2018). Pericentromere-Specific Cohesin Complex Prevents Meiotic Pericentric DNA Double-Strand Breaks and Lethal Crossovers. *Mol Cell. 71*: 540–553.

Nichols, B.A., Oswald, N.W., McMillan, E.A., McGlynn, K., Yan, J., Kim, M.S., Saha, J., Mallipeddi, P.L., LaDuke, S.A., Villalobos, P.A., Rodriguez-Canales, J., Wistuba, I.I., Posner, B.A., Davis, A.J., Minna, J.D., MacMillan J.B., Whitehurst, A.W. (2018). HORMAD1 is a negative prognostic indicator in lung adenocarcinoma and specifies resistance to oxidative and genotoxic stress. *Cancer Res. 78*: 6196-6208.

Ning, Y., Liu, Q., Wang, C., Qin, E., Wu, Z., Wang, M., Yang, K., Elesawi, I.E., Chen, C., Liu, H., Qin, R., Liu, B. (2021). Heat stress interferes with formation of double-strand breaks and homolog synapsis. *Plant Physiol. 185*: 1783-1797.

Oshino, T., Abiko, M., Saito, R., Ichiishi, E., Endo, M., Kawagishi-Kobayashi, M., Higashitani, A. (2007). Premature progression of anther early developmental programs accompanied by comprehensive alterations in transcription during high-temperature injury in barley plants. *Mol Genet Genomics. 278*: 31–42.

Otto, S.P., Payseur, B.A. (2019). Crossover Interference: Shedding Light on the Evolution of Recombination. *Annu Rev Genet. 53*: 19-44.

Page, S.L., Hawley, R.S. (2001). c(3)G encodes a Drosophila synaptonemal complex protein. *Genes Dev. 15*: 3130–3143.

Panizza, S., Mendoza, M.A., Berlinger, M., Hunag, L., Nicolas, A., Shirahige, K., Klein, F. (2011). SPO11-accessory proteins link double strand break sites to the chromosome axis in early meiotic recombination. *Cell. 146*: 372-83.

Parvanov, E.D., Petkov, P.M., Paigen, K. (2010). Prdm9 controls activation of mammalian recombination hotspots. *Science. 327:* 835.

Pratto, F., Brick, K., Cheng, G., Lam, K-W.G., Cloutier, J.M., Dahiya, D., Wellard, S.R., Jordan, P.W., Camerini-Otero, R.D. (2021). Meiotic recombination mirrors patterns of germline replication in mice and humans. *Cell. 184:* 4251-4267.

Pawlowski, W.P., Golubovskaya, I.N., Cande, W.Z. (2003). Altered nuclear distribution of recombination protein RAD51 in maize mutants suggests the involvement of RAD51 in meiotic homology recognition. *Plant Cell. 15*: 1807-16.

Rasmussen, S.W. (1977). Meiosis in Bombyx mori females. *Philos Trans R Soc Lond B Biol Sci. 277*: 343-50.

Rog, O., Köhler, S., Dernburg, A.F. (2017). The synaptonemal complex has liquid crystalline properties and spatially regulates meiotic recombination factors. *eLife. 6*: e21455.

Roig, I., Dowdle, J.A., Toth, A., de Rooij, D.G., Jasin, M., Keeney, S. (2010). Mouse TRIP13/PCH2 is required for recombination and normal higher-order chromosome structure during meiosis. *PLoS Genet. 6*: e1001062.

Rousová, D., Nivsarkar, V., Altmannova, V., Raina, V.B., Funk, S.K., Liedtke, D., Janning, P., Müller, F., Reichle, H., Vader, G., Weir, J. (2021). Novel mechanistic insights into the role of Mer2 as the keystone of meiotic DNA break formation. *Elife. 10:* e72330.

Sanchez-Moran, E., Santos, J-L., Jones, G.H., Franklin, F.C.H. (2007). ASY1 mediates AtDMC1-dependent interhomolog recombination during meiosis in Arabidopsis. *Genes Dev. 21:* 2220-2233.

Schalbetter, S.A., Fudenberg, G., Baxter, J., Pollard, K.S., Neale, M.J. (2019). Principles of meiotic chromosome assembly revealed in S. cerevisiae. *Nat Commun. 10*: 4795.

Schild-Prüfert, K., Saito, T.T., Smolikov, S., Gu, Y., Hincapie, M., Hill, D.E., Vidal, M., McDonald, K., Colaiácovo, M.P. (2011). Organization of the synaptonemal complex during meiosis in Caenorhabditis elegans. *Genetics. 189*: 411-421.

Schwacha, A., Kleckner, N. (1994). Identification of joint molecules that form frequently between homologs but rarely between sister chromatids during yeast meiosis. *Cell. 76*: 51-63.

Schwacha A., Kleckner, N. (1997). Interhomolog bias during meiotic recombination: meiotic functions promote a highly differentiated interhomolog only pathway. *Cell. 90*: 1123-35.

Severson, A.F., Ling, L., van Zuylen, V., Meyer, B.J. (2009). The axial element protein HTP-3 promotes cohesin loading and meiotic axis assembly in C. elegans to implement the meiotic program of chromosome segregation. *Genes Dev. 23*: 1763-78.

Severson, A.F., Meyer, B.J. (2014). Divergent kleisin subunits of cohesin specify mechanisms to tether and release meiotic chromosomes. *Elife. 3*: e03467.

Shahzad, M.M.K., Shin, Y.H., Matsuo, K., Lu, C., Nishimura, M., Shen, D.Y., Kang, Y., Hu, W., Mora, E.M., Rodriguez-Aguayo, C., Kapur, A., Bottsford-Miller, J., Lopez-Berestein, G., Rajkovic, A., Sood, A.K. Biological significance of HORMA domain containing protein 1 (HORMAD1) in epithelial ovarian carcinoma. *Cancer Lett. 330*: 123-129.

Shi, J., Wolf, S.E., Burke, J.M., Presting, G.G., Ross-Ibarra, J., Dawe, R.K. (2010). Widespread gene conversion in centromere cores. *PLoS Biol. 8*: e1000327.

Shin, Y-H., Choi, Y., Erdin, S.U., Yatsenko, S.A., Kloc, M., Yang, F., Wang, J., Meistrich, M.L., Rajkovic, A. (2010). Hormad1 mutation disrupts synaptonemal complex formation, recombination, and chromosome segregation in mammalian meiosis. *PLoS Genet. 6*:e1001190.

Shodhan, A., Kataoka, K., Mochizuki, K., Novatchkova, M., Loidl, J. (2017). A Zip3-like protein plays a role in crossover formation in the SC-less meiosis of the protist Tetrahymena. *Mol Biol Cell. 28*: 825–833.

Simpson, A.J., Caballero, O.L., Jungbluth, A., Chen, Y.T., Old, L.J. (2005). Cancer/testis antigens, gametogenesis and cancer. *Nat Rev Cancer. 5*: 615-625.

Sommermeyer, V., Béneut, C., Chaplais, E., Serrentino, M.E., Borde, V. (2013). Spp1, a member of the Set1 complex, promotes meiotic DSB formation in promoters by tethering histone H3K4 methylation sites to chromosome axes. *Mol Cell. 49:* 43-54.

Stanzione, M., Baumann, M., Papanikos, F., Dereli, I., Lange, J., Ramlal, A., Tränkner, D., Shibuya, H., de Massy, B., Watanabe, Y., Jasin, M., Keeney, S., Tóth, A. (2016). Meiotic DNA break formation requires the unsynapsed chromosome axis-binding protein IHO1 (CCDC36) in mice. *Nat Cell Biol. 18:* 1208-1220.

Sturtevant, A.H. (1915). The behavior of the chromosomes as studied through linkage. *Zeitschrift für Induktive Abstammungs- und Vererbungslehre. 13*: 234-287.

Sun, X., Huang, L., Markowitz, T.E., Blitzblau, H.G., Chen, D., Klein, F., Hochwagen, A. (2015). Transcription dynamically patterns the meiotic chromosome-axis interface. *Elife. 4*: e07424.

Sym, M., Roeder, G.S. (1994). Crossover interference is abolished in the absence of a synaptonemal complex protein. *Cell. 79:* 283-292.

Takemoto, K., Tani, N., Takada-Horisawa, Y., Fujimura, S., Tanno, N., Yamane, M., Okamura, K., Sugimoto, M., Araki, K., Ishiguro, K-I. (2020). Meiosis-specific C19orf57/4930432K21Rik/BRME1 modulates localization of RAD51 and DMC1 to DSBs in mouse meiotic recombination. *Cell Rep. 31:* 107686.

Tedeschi, A., Wutz, G., Huet, S., Jaritz, M., Wuensche, A., Schirghuber, E., Davidson, I.F., Tang, W., Cisneros, D.A., Bhaskara, V., Nishiyama, T., Vaziri, A., Wutz, A., Ellenberg, J., Peters, J.M. (2013). Wapl is an essential regulator of chromatin structure and chromosome segregation. *Nature. 501*: 564-8.

Valuchova,, S., Mikulkova, P., Pecinkova, J., Klimova, J., Krumnikl, M., Bainar, P., Heckmann, S., Tomancak, P., Riha, K. (2020). Imaging plant germline differentiation within Arabidopsis flowers by light sheet microscopy. *Elife. 9*: e52546.

Vrielynck, N., Schneider, K., Rodriguez, M., Sims, J., Chambon, A., Hurel, A., De Muyt, A., Ronceret, A., Krsicka, O., Mézard, C., Schlögelhofer, P., Grelon, M. (2021). Conservation and divergence of meiotic DNA double strand break forming mechanisms in Arabidopsis thaliana. *Nucleic Acids Res. 49:* 9821-9835.

Walker, J., Gao, H., Zhang, J., Aldridge, B., Vickers, M., Higgins, J.D., Feng, X. (2018). Sexual-lineage-specific DNA methylation regulates meiosis in Arabidopsis. *Nat Genet. 50*: 130-137.

Wang, X., Tan, Y., Cao, X., Kim, J.A., Chen, T., Hu, Y., Wexler, M., Wang, X. (2018). Epigenetic activation of HORMAD1 in basal-like breast cancer: role in Rucaparib sensitivity. *Oncotarget. 9*: 30115-30127.

Wang, Y., Zhai, B., Tan, T. Yang, X., Zhang, J., Song, M., Tan, Y., Yang, X., Chu, T., Zhang, S., Wang, S., Zhang, L. (2021). ESA1 regulates meiotic chromosome axis and crossover frequency via acetylating histone H4. *Nucleic Acids Res. 49*: 9353-9373.

Ward, A., Hopkins, J., Mckay, M., Murray, S., Jordan, P.W. (2016). Genetic interactions between the meiosis-specific cohesin components, STAG3, REC8, and RAD21L. *G3 (Bethesda). 6:* 1713-1724.

Watanabe, Y., Yokobayashi, S., Yamamoto, M., Nurse, P. (2001). Pre-meiotic S phase is linked to reductional chromosome segregation and recombination. *Nature 409*: 359-63.

West, A. M. V., Komives, E. A., & Corbett, K. D. (2018). Conformational dynamics of the Hop1 HORMA domain reveal a common mechanism with the spindle checkpoint protein Mad2. *Nucleic Acids Res*. *46*: 279–292.

West, A. M., Rosenberg, S. C., Ur, S. N., Lehmer, M. K., Ye, Q., Hagemann, G., Caballero, I., Usón, I., MacQueen, A. J., Herzog, F., & Corbett, K. D. (2019). A conserved filamentous assembly underlies the structure of the meiotic chromosome axis. *ELife*. 8: e40372.

Wojtasz, L., Cloutier, J.M., Baumann, M., Daniel, K., Varga, J., Fu, J., Anastassiadis, K., Stewart, A.F., Reményi, A., Turner, J.M.A., Tóth, A. (2012). Meiotic DNA double-strand breaks and chromosome asynapsis in mice are monitored by distinct HORMAD2-independent and -dependent mechanisms. *Genes Dev. 26*: 958-73.

Wright, K.M., Arnold, B., Xue, K., Šurinová, M., O'Connell, J., Bomblies, K. (2015). Selection on meiosis genes in diploid and tetraploid Arabidopsis arenosa. *Mol biol Evol. 32*: 944–955.

Yan, R., McKee, B.D. (2013). The cohesion protein SOLO associates with SMC1 and is required for synapsis, recombination, homolog bias and cohesion and pairing of centromeres in Drosophila meiosis. *PLoS Genet. 9:* e1003637

Yang, C., Hu, B., Portheine, S.M., Chuenban, P., Schnittger, A. (2020a). State changes of the HORMA protein ASY1 are mediated by an interplay between its closure motif and PCH2. *Nucleic Acids Res. 48*: 11521-11535.

Yang, C., Sofroni, K., Wijnker, E., Hamamura, Y., Carstens, L., Harashima, H., Stolze, S.C., Vezon, D., Chelysheva, L., Orban-Nemeth, Z., Pochon, G., Nakagami, H., Schlögelhofer, P., Grelon, M., Schnittger, A. (2020b). The Arabidopsis Cdk1/Cdk2 homolog CDKA;1 controls chromosome axis assembly during plant meiosis. *EMBO J. 39*: e101625.

Yoon, S., Choi, E-H., Kim, J-W., Kim, K.P. (2018). Structured illumination microscopy imaging reveals localization of replication protein A between chromosome lateral elements during mammalian meiosis. *Exp Mol Med. 50*: 1-12.

Yuan, L., Liu, J.G., Zhao, J., Brundell, E., Daneholt, B., Höög, C. (2000). The murine SCP3 gene is required for synaptonemal complex assembly, chromosome synapsis, and male fertility. *Mol Cell. 5*: 73-83.

Zhang, L., Espagne, E., de Muyt, A., Zickler, D., Kleckner, N.E., 2014a. Interference-mediated synaptonemal complex formation with embedded crossover designation. *Proc Natl Acad Sci USA. 111*: E5059–E5068.

Zhang, J., Gurusaran, M., Fujiwara, Y., Zhang, K., Echbarthi, M., Vorontsov, E., Guo, R., Pendlebury, D.F., Alam, I., Livera, G., Emmanuelle, M., Wang, P.J., Nandakumar, J., Davies, O.R., Shibuya, H. (2020). The BRCA2-MEILB2-BRME1 complex governs meiotic recombination and impairs the mitotic BRCA2-RAD51 function in cancer cells. *Nat Commun. 11:* 2055.

Zhang, L., Liang, Z., Hutchinson, J., Kleckner, N. (2014b). Crossover Patterning by the Beam-Film Model: Analysis and Implications. *PLoS Genetics. 10*: e1004042.

Zhang, L., Wang, S., Yin, S., Hong, S., Kim, K.P., Kleckner, N. (2014c). Topoisomerase II mediates meiotic crossover interference. *Nature 511*: 551–556.

Zhang, Z., Xie, S., Wang, R., Guo, S., Zhao, Q., Nie, H., Liu, Y., Zhang, F., Chen, M., Liu, L., Meng, X., Liu, M., Zhao, L., Colaiácovo, M.P., Zhou, J., Gao, J. (2020). Multivalent weak interactions between assembly units drive synaptonemal complex formation. *J Cell Biol. 219*: e201910086.

Zickler, D., Klecker, N. (1999). Meiotic chromosomes: integrating structure and function. *Annu Rev Genet. 33*: 603-754.

Ziolkowski, P.A., Underwood, C.J., Lambing, C., Martinez-Garcia, M., Lawrence, E.J., Ziolkowska, L., Griffin, C., Choi, K., Franklin, F.C.H., Martienssen, R.A., Henderson, I.R. (2017). Natural variation and dosage of the HEI10 meiotic E3 ligase control Arabidopsis crossover recombination. *Genes Dev. 31*: 306-317

Zuo, W, Chen, G., Gao, Z., Li, S., Chen, Y., Huang, C., Chen, J., Chen, Z., Lei, M., Bian, Q. (2021). Stage-resolved Hi-C analyses reveal meiotic chromosome organizational features influencing homolog alignment. *Nat. Commun. 12*: 5827.

Table 1. Functions of chromosome axis proteins in the formation of DSBs and COs across species

Mutants	Species	DSB formation	CO formation	References
Coiled coil proteins				
red1	*S. cerevisiae*	- Strong reduction in DSBs - Near abolishment of Rec114 and Mer2 binding to the chromatin genome-wide	- Reduction of interhomolog joint molecules and COs	Kim et al. 2010 Panizza et al. 2011 Schwacha and Kleckner 1997
rec10	*S. pombe*	- Detectable DSBs at only one hotspot at approximately 1% of the wild type level	- Severe reduction in CO formation	Ellermeier and Smith, 2005 Fowler et al. 2013
rec25	*S. pombe*	- Differential DSB reduction	- Region-specific reduction in CO formation	Fowler et al. 2013 Martin-Castellanos et al. 2005
rec27	*S. pombe*	- Differential DSB reduction	- Region-specific reduction in CO formation	Fowler et al. 2013

				Martin-Castellanos et al. 2005
mug20	*S. pombe*	- Differential DSB reduction	- Region-specific reduction in CO formation	Estreicher et al. 2012 Fowler et al. 2013
Sycp2	*M. musculus*	- Slight reduction in RAD51 foci number in spermatocytes - Less IHO1 foci co-localising with SMC3-stained axis	- Unknown. Meiotic arrest and cellular apoptosis prevent the study of late stages with CO markers	Fujiwara et al. 2020
Sycp3	*M. musculus*	- Reduction in RAD51 and DMC1 foci in spermatocytes	- Unknown. Meiotic arrests and cellular apoptosis prevent the study of late stages with CO markers	Yuan et al. 2000
asy3	*A. thaliana*	- 29.0% less γH2AX foci - 25.7% less DMC1 foci - 29.2% less RAD51 foci	- 66.2% less chiasmata - Influences class I and class II COs	Ferdous et al. 2012 Vrielynck et al. 2021

		- 21.6% less MSH4 foci - 77.2% less PRD3 foci		
asy4	*A. thaliana*	- No defect in DMC1 or MSH5 foci number	- 33.7% less chiasmata. - Influences class I and class II COs - Regional effect: 3 genetic intervals show a reduction in recombination frequency, 1 genetic interval shows an increase in recombination frequency	Chambon et al. 2018
dsy2	*Z. mays*	- 70.0% less RAD51 foci - Reduction of Tunnel assay signal	- 75.6% less bivalent chromosomes. Unknown effect on class I or class II COs	Lee et al. 2015
HORMA proteins				
hop1	*S. cerevisiae*	- Strong reduction in DSBs	- Reduction of interhomolog	Panizza et al. 2011

		- Near abolishment of Rec114 binding to the chromatin genome-wide	joint molecules and COs	Schwacha and Kleckner 1994
hop1	*S. pombe*	- Reduction of DSBs - Reduction of RAD51 foci	- Reduction of CO frequency	Latypov et al. 2010 Lorenz et al. 2006
Hormad1	*M. musculus*	- 90.6% less DMC1 foci in spermatocytes - 63.4% less RAD51 foci in spermatocytes - 64.0% less RPA foci in spermatocytes - Reduction of MSH4 foci in spermatocytes - Reduction to 2- to 4.8-fold in testis-weight-normalized SPO11-oligonucleotide level	- Reduction in the number of MLH1 foci in spermatocytes - 70% less MLH1 foci in oocytes	Daniel et al. 2011 Shin et al. 2010 Stanzione et al., 2016

		- 62.1% less DMC1 foci in oocytes - 57.0% less RAD51 foci in oocytes - 83.7% less RPA foci in oocytes - Reduced level of IHO1		
Hormad2	*M. musculus*	- Slight reduction in DMC1 and RAD51 foci in spermatocytes	- No change in MLH1 foci in oocytes	Wojtasz et al. 2012
asy1	*A. thaliana*	- No difference in γH2AX foci - 66.0% less PRD3 foci	- 80.7% less chiasmata. - Influence class I and class II COs.	Cuacos et al. 2021 Sanchez-Moran et al. 2007 Vrielynck et al. 2021
asy1	*Brassica rapa*	- Not reported	- 80.7% less chiasmata. - Influences class I COs. Unknown effect on class II COs.	Cuacos et al. 2021
asy1	*Triticum aestivum*	- Not reported	- Partial loss of chiasmata and	Boden et al. 2009

			presence of multivalent chromosomes in *asy1* down-regulated line	
him-3	*C. elegans*	- No defect in RAD51 foci count or localization	- Defect in inter-homolog recombination	Couteau et al. 2004 Couteau et al. 2005
htp-1	*C. elegans*	- 70% less RAD-51 foci - 23-fold increase in RAD-51 foci in *htp-1 him-3* compared to *htp-1* - 12-fold increase in RAD-51 foci in *htp-1 htp-2* compared to *htp-1*	- 85% less bivalent chromosomes at diakinesis - Absence of bivalent chromosome in *htp-1 htp2* - Reduction of 75% recombination frequency in a large genetic interval on the left arm of the X chromosome	Couteau et al. 2005 Martinez-Perez and Villeneuve 2005
htp-2	*C. elegans*	- 12-fold increase in RAD-51 foci in *htp-1 htp-2* compared to *htp-*	- Absence of bivalent chromosome in *htp-1 htp2*	Couteau et al. 2005

		1 but below wild type level		
htp-3	*C. elegans*	- Absence of RAD-51 foci - Absence of RPA-1 foci	- Only univalent chromosomes	Goodyer et al. 2008
Kleisins				
rec8	*S. cerevisiae*	- Redistribution of Rec114 genome-wide - Differential localization of SPO11 - Region specific reduction in DSB formation	- No effect on the inter-homolog bias on single-end invasions - Inter-homolog bias is reduced on double Holliday Junctions and CO rate is reduced	Kim et al. 2010 Kugou et al. 2009 Panizza et al. 2011 Klein et al., 1999
rec8	*S. pombe*	- Low level of DSBs at some hotspots	- Region specific reduction in CO formation	Ellermeier and Smith, 2005 Fowler et al. 2013
rec8	*M. musculus*	- 23% less DMC1 foci number in spermatocytes - IHO1 localisation is restricted to the	- Unknown. Meiotic arrests and cellular apoptosis prevent the study of late	Bhattacharyya et al. 2019

		shorter SYCP3-stained axis	stages with CO markers	
rad21l	*M. musculus*	- 34% less DMC1 foci number in spermatocytes	- Unknown. Meiotic arrests and cellular apoptosis prevent the study of late stages with CO markers	Bhattacharyya et al. 2019
rec8/syn1	*A. thaliana*	- 73.8% less γH2AX foci - 80.2% less RAD51 foci - 77.4% less RPA1a foci - 91.7% less DMC1 foci - 92.5% less MSH4 foci	- 52.9% less MLH1 foci	Lambing et al. 2020b
afd1	*Z. mays*	- 89.4% less RAD51 foci	- Presence of univalent chromosomes	Pawlowski et al. 2003
rec-8	*C. elegans*	- RAD51 present in *rec-8* but abolished in *rec-8 coh-3 coh-4*	- Presence of univalent chromosomes	Severson et al. 2009 Severson and Meyer 2014
coh-3	*C. elegans*	- RAD51 present in *rec-8* but	- Presence of univalent	Severson et al. 2009

		abolished in *rec-8 coh-3 coh-4*	chromosomes in *coh-3 coh-4*	Severson and Meyer 2014
coh-4	*C. elegans*	- RAD51 present in *rec-8* but abolished in *rec-8 coh-3 coh-4*	- Presence of univalent chromosomes in *coh-3 coh-4*	Severson et al. 2009 Severson and Meyer 2014
c(2)m	*D. melanogaster*	- Reduction of γH2Av foci	- Reduction in recombination frequency at several genetic intervals	Manheim and McKim 2003 Mehrotra and McKim 2006
solo	*D. melanogaster*	- No change in γH2Av foci	- Reduction in chiasma number	Yan and McKee, 2013

Figures

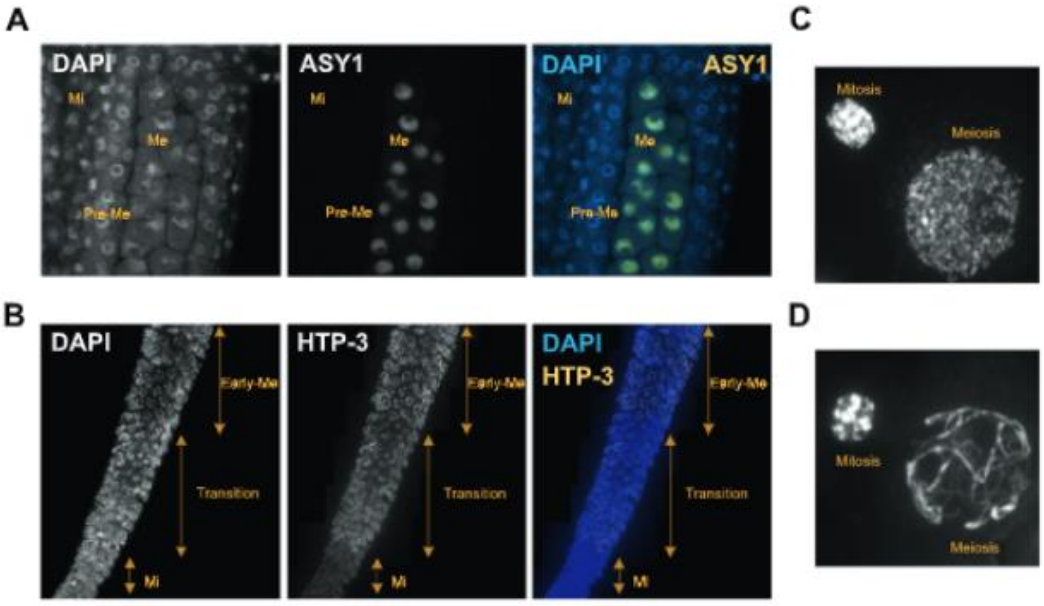

E

S. cerevisiae	*Hop1* 1030.0 / 1.4	*Red1* 412.6 / 37.8	*Rec8* 874.1 / 8.7	*RAD61 (Wapl-like)* 92.1 / 41.8	*PDS5* 321.5 / 54.3							
S. pombe	*Hop1* Ratio: 4.4	*Rec10* Ratio: 14.9	*Rec25* Ratio: 4.9	*Rec27* Ratio: 1.1	*Mug20* Ratio: 8.8	*Rec8* Ratio: 16.4	*Wpl1* Ratio: 1.6	*Pds5* Ratio: 2.0				
A. thaliana	*ASY1* 37.9 / 0.0	*ASY2* 0.4 / 0.2	*ASY3* 30.2 / 0.2	*ASY4* 77.1 / 0.1	*REC8* 27.9 / 0.0	*WAPL 1* 6.9 / 0.4	*WAPL 2* 6.9 / 0.5	*PDS5a* 14.2 / 3.8	*PDS5b* 11.3 / 0.4	*PDS5c* 10.4 / 1.9	*PDS5d* 7.92 / 0.78	*PDS5 e* 4.08 / 0.83
Z. mays	*ASY1* 8569.1 / 920.4	*ASY3* 876.6 / 88.7	*ASY4* 2011.9 / 217.8	*REC8* 13147.3 / 556.2	*WAPL 1* 185.1 / 349.1	*WAPL 2* 1009.6 / 937.9	*WAPL 3* 966.5 / 1468.0	*PDS5* 2074.2 / 2876.4				
H. vulgare	*ASY1* 178.3 / 0.7	*ASY3.1* 0.2 / 0.0	*ASY3. 2* 29.9 / 0.1	*ASY3.3* 15.6 / 5.4	*ASY4.1* 10.9 / 1.2	*ASY4. 2* 97.0 / 8.1	*REC8.1* 69.7 / 6.8	*REC8.2* 26.5 / 3.8	*WAPL 1* 0.8 / 0.3	*WAPL 2* 0.9 / 1.4	*WAPL 3* 36.1 / 22.9	
D. melanogaster	*C(2)M* 5.1 / 0.1											
C. elegans	*HTP-1* 133.5 / 3.9	*HTP-2* 105.9 / 1.3	*HTP-3* 41.1 / 2.4	*HIM-3* 186.0 / 2.6	*REC-8* 39.8 / 2.2	*COH-3* 11.1 / 1.3	*COH-4* 14.2 / 0.8					
M. musculus	*HORMAD1* 91.0 / BC	*HORMAD2* 21.0 / BC	*SYCP2* 201.0 / BC	*SYCP3* 173.8 / 9.0	*REC8* 127.0 / 8.7	*RAD21* 77.0 / 149.0	*RAD21 L* 6.0 / BC	*WAPL* 85.0 / 49.0	*PDS5a* 10.0 / 10.0	*PDS5b* 20.0 / 15.0		

Figure 1. Comparison in gene expression and cell size between mitosis and meiosis

(**A**) Section of an *A. thaliana* bud. Chromatin is stained with DAPI (white or blue). ASY1-eYFP (white or yellow) is detected directly under a confocal microscope. Mi: mitosis; Pre-Me: pre-meiosis; Me: meiosis. Note the difference in cell and chromatin sizes between mitosis and

meiosis. Image courtesy of Sebastien Andreuzza (**B**) Section of a *C. elegans* gonad. Chromatin is stained with DAPI (white or blue). HTP-3 is immunostained on chromosomes (white or yellow). Mi: mitosis; Transition: transition zone; Early-Me: early meiosis. Note the difference in chromatin size between mitosis and meiosis. Image courtesy of Chloé Girard. (**C**) Chromosome spread of tomato nuclei from inflorescence buds containing a mixture of somatic and meiotic cells. On the left side is a mitotic cell and on the right side is a meiotic cell in early prophase I. Chromatin is stained with DAPI. Note the difference in chromatin size between the mitotic and meiotic cells. (**D**) Chromosome spread of tomato nuclei from inflorescence buds containing a mixture of somatic and meiotic cells. On the left side is a mitotic cell and on the right side is a meiotic cell in mid prophase I. Chromatin is stained with DAPI. Note the change in chromatin conformation and the formation of a dense linear structure (synaptonemal complex). (**E**) Gene expression of axis proteins in meiotic and somatic cells. *S. cerevisiae* (meiosis vs vegetative stage; RNAseq; Reads Per Million reads (RPM) (Brar et al., 2012)), *S. pombe* (ratio is meiotic RNA level divided by vegetative RNA level; microarray data (http://www.bahlerlab.info/resources)), *A. thaliana* (isolated meiocyte vs leaf; RNAseq; Transcripts Per Million (TPM) (Walker et al., 2018)), *Z. mays* (isolated meiocyte vs seedling; RNAseq; RPM (Dukowic-Schulze et al., 2014)), *H. vulgare* (isolated meiocyte vs germinating embryo; RNAseq; TPM (Barakate et al., 2021)), *D. melanogaster* (ovary vs spermatheca; RNAseq; Fragments Per Kilobase of transcript per Million mapped reads (FPKM) (http://flyatlas.gla.ac.uk/FlyAtlas2/)), *C. elegans* (ovary vs larvae; RNAseq; FPKM (https://wormbase.org/)), *M. musculus* (meiosis vs kidney; RNAseq; TPM (http://www.ebi.ac.uk/gxa/)). Genes coding for HORMA-domain containing proteins are in blue, coiled-coil proteins in orange, kleisins in green, and cohesin regulators in purple. “n.d.” means “not determined".

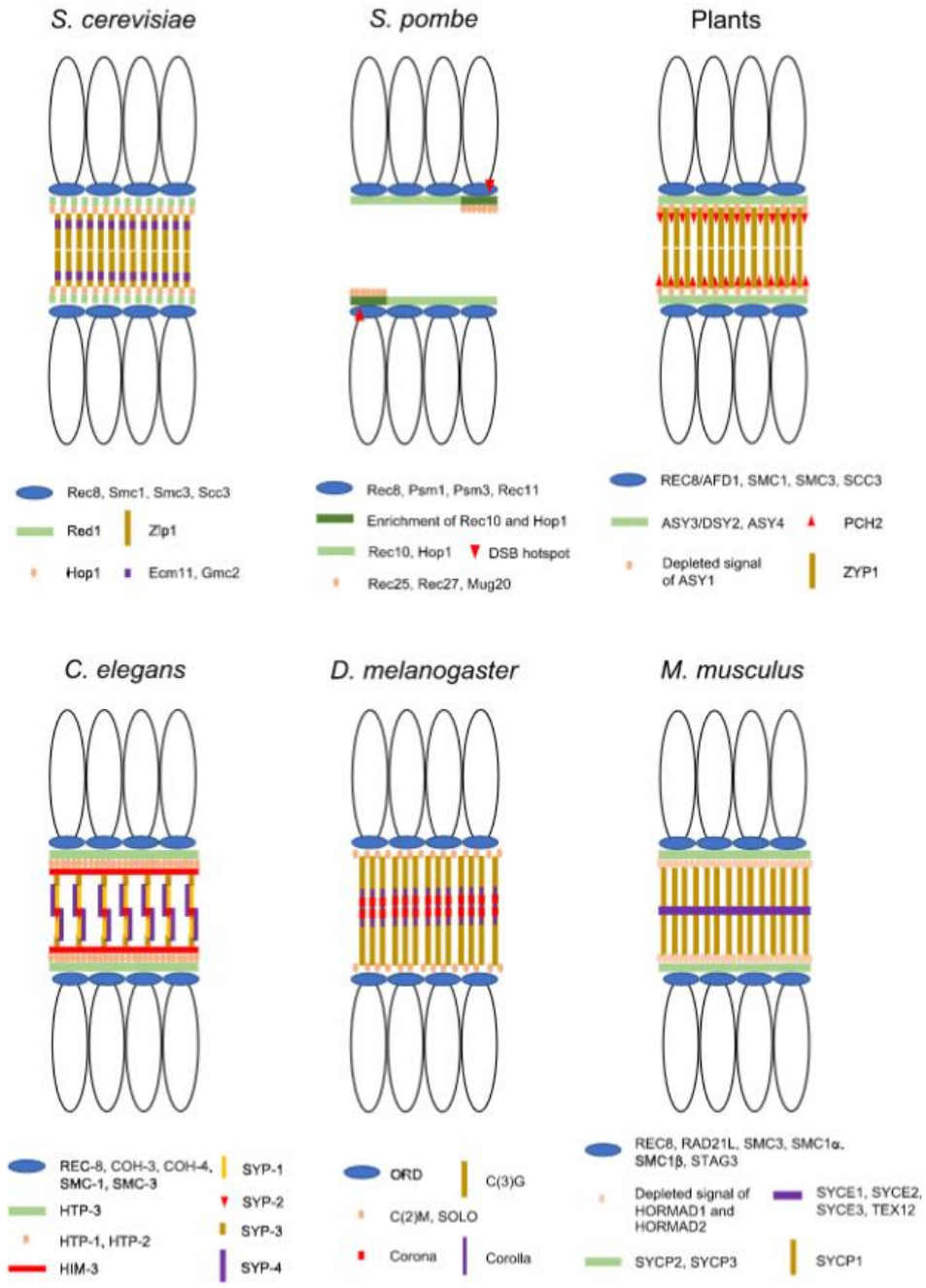

Figure 2. Composition of the meiotic chromosome axis across species

Schematic representation of the meiotic chromosome axis in ***S. cerevisiae*** (Humphryes et al., 2013; Panizza et al., 2011), ***S. pombe*** (Fowler et al., 2013; Kariyazono et al., 2019), ***C. elegans*** (Köhler et al. 2017; Schild-Prüfert et al., 2011), ***D. melanogaster*** (Anderson et al., 2005; Cahoon et al., 2017), ***M. musculus*** (Fujiwara et al., 2020; Roig et al., 2010; Yoon et al., 2018) and **plant** (Lambing et al., 2015; Miao et al., 2013). For data leading to these models, see the indicated references.

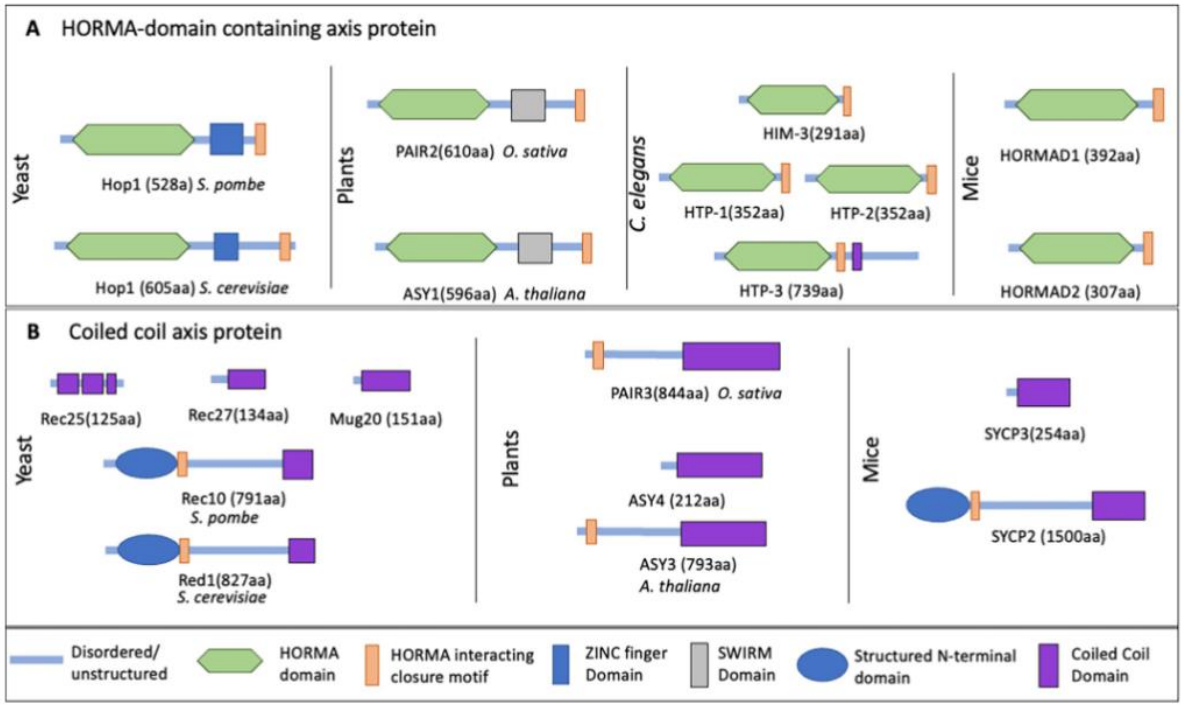

Figure 3. Domain architecture of meiotic axis proteins.

Schematic representation depicting variation in length and domain architecture of **(A)** HORMA- domain containing proteins (HORMADs), **(B)** Coiled-coil axis proteins from species belonging to different kingdoms. Representations are made based on data from PDB and AlphaFold databases.

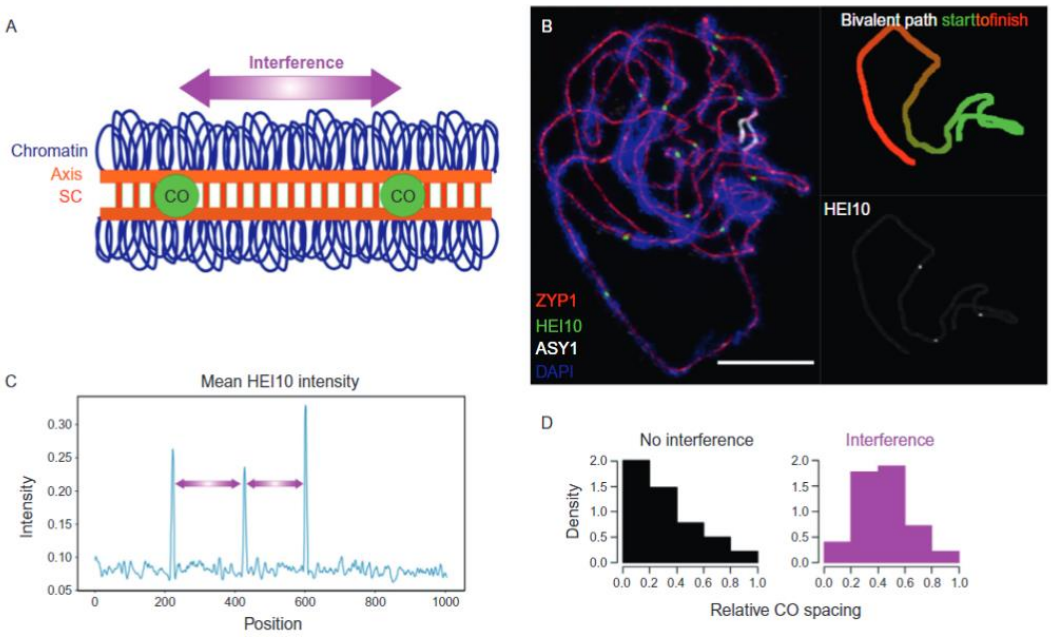

Figure 4. CO interference.

(A) Cartoon showing the structure of a meiotic pachytene bivalent. CO interference inhibits COs from forming too close together along the length of the bivalent. **(B)** An example of an *A. thaliana* late-pachytene nucleus stained for ZYP1 (red), HEI10 (green), ASY1 (white) and DAPI (blue). Scale bar = 5 µm. Late HEI10 foci mark CO sites in *A. thaliana* and can be cytologically mapped along individual bivalents using the approach from Morgan et al., 2021a. The orientation of a segmented bivalent from the example nucleus is shown along with the bivalent path's HEI10 channel. **(C)** Plot of the mean HEI10 intensity along the bivalent path from (B). Interference (signified by magenta arrows) prevents late-HEI10 foci from forming too close to one another. **(D)** Histograms comparing the expected spacing between adjacent COs if there was no interference (black) and CO spacing along *A. thaliana* bivalents (magenta, data from Morgan *et al.,* 2021a).

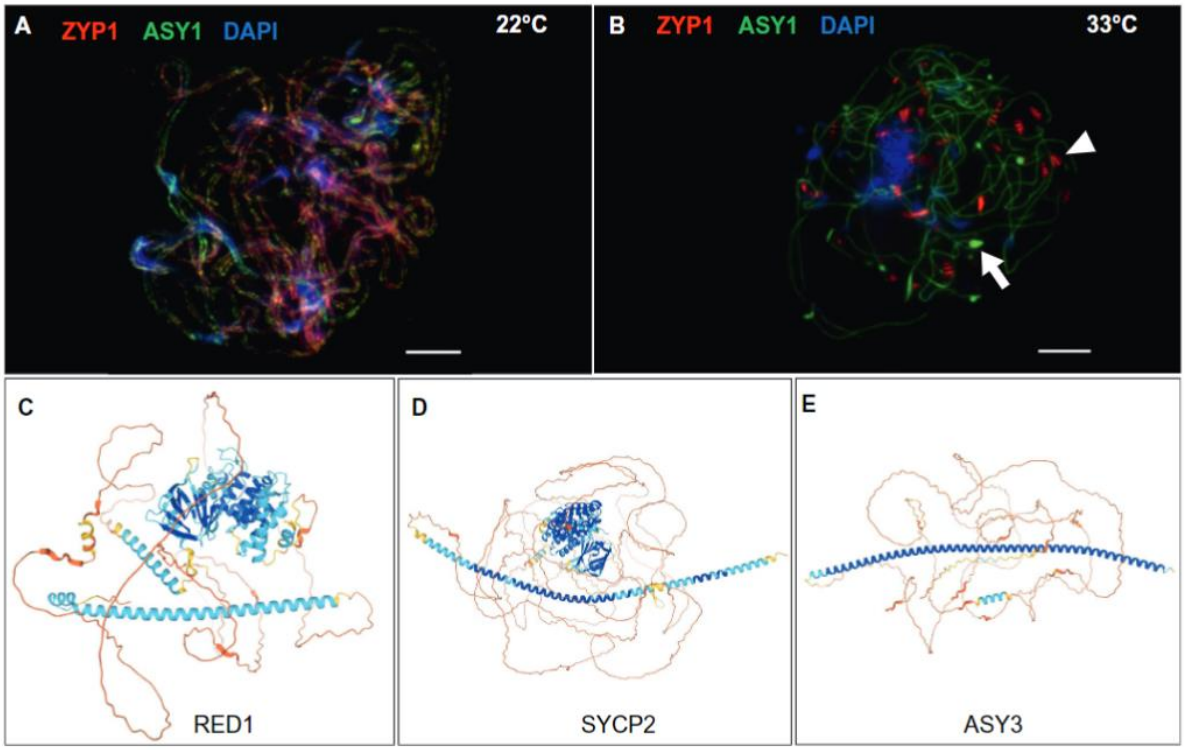

Figure 5. Temperature and axis proteins.

(A,B) Examples of autotetraploid *Arabidopsis arenosa* prophase I nuclei from plants grown at 22°C **(A)** and 33°C **(B)**. Nuclei are stained for ZYP1 (red), ASY1 (green) and DAPI (blue). The white arrow shows an example of an ASY1 aggregate and the white arrowhead shows an example of a ZYP1 polycomplex. Scale bars = 5 μm. **(C-E)** Structure of axis proteins predicted by AlphaFold (https://alphafold.ebi.ac.uk) for *S. cerevisiae* Red1 **(C),** human SYCP2 **(D)** and *A. thaliana* ASY3 (**E**). Color code is used for depicting the per residue confidence score (pLDDT) which is an indicator of confidence in predicted secondary structure for each residue in a protein. Dark blue codes for confidence greater than 90%, light blue for between 70% and 90%, yellow for between 50% and 70%, while orange for less than 50%.

Acknowledgement

We thank Sebastien Andreuzza and Chloé Girard for providing images of *A. thaliana* buds and *C. elegans*, respectively; Abdellah Barakate, Changbin Chen and Gloria Brar for providing the expression of axis genes in *H. vulgare*, *Z. mays*, and *S. cerevisiae*, respectively; and Scott Keeney for fruitful discussions.

CM is supported by a BBSRC Discovery Fellowship (BB/V005774/1). NH research is funded by JSPS KAKENHI Grant Numbers JP23591836, JP25125705, JP26461881, JP16H01298, JP17K10471, and JP20K08127 and by grants from the Takeda Science Foundation and the Naito Foundation. GRS research is funded by grant R35 GM118120 from the National Institutes of Health of the United States of America. CL research is funded by a BBSRC grant-aided support as part of the Institute Strategic Program Designing Future Wheat Grant (BB/P016855/1) and an Institutional Sponsorship fund as part of the UKRI grant (BB/W510543/1).